The Planes of Satellite Galaxies

Jessica Kocher

Lund Observatory
Lund University

2022-EXA188

Degree project of 15 higher education credits
January 2022

Supervisor: Oscar Agertz

Lund Observatory
Box 43
SE-221 00 Lund
Sweden

Abstract

The Planes of Satellites Problem is an open question within the field of galaxy formation. It is based on the observations that the Milky Way's satellites, as well as those around the Andromeda (M31) galaxy, align in planes. This applies both to the satellites' positions lying close to the plane of best fit, and to the satellites' orbital planes aligning within a narrow angle. Such planar structures are not predicted by the standard model of cosmology, Λ Cold Dark Matter (ΛCDM). Simulations based on this model only very rarely reproduce planes as thin and orbitally aligned as those we observe.

In this project, we worked with five hydrodynamical simulations to study the planarity of each host-satellites system using both a spatial (plane height) and a kinematic metric (orbital dispersion). Two of the five simulations represent general cosmological simulations, while the remaining three form a set specifically modified to include a major merger of a given mass ratio. This allowed me to test whether the size of past mergers influence the formation of satellite planes. In all cases, we compared the five simulations to each other and the observed systems, as well as to isotropic realizations, both with randomized radial distributions and radial values corresponding to each simulation's satellite distribution. While the analysis focused on a single instance near $z = 0$ from each simulation, we considered a longer time span in one simulation to obtain an impression of the longevity of a plane.

From our results, we argue that all five simulations can be considered significantly planar, at least if the number of member galaxies belonging to the planes is kept variable. The small sample size makes it impossible to make generalizations concerning how common planes are in ΛCDM overall, but the presented cases certainly show that systems comparable to the Milky Way or M31 are possible within the standard theory. We further found a plane that was nearly static in both spatial and kinematic metrics across 341 Myr, although further analysis would be needed to establish how long-lived the plane is and how common such stable planes are in the ΛCDM framework. Lastly, the modified suite of simulations displayed a monotonic trend in which a larger major merger corresponded to a thinner and more orbitally aligned plane in the resulting system.

Populärvetenskaplig beskrivning

The planes of satellite galaxies problem is a hotly debated topic in the research field of galaxy formation. This problem is concerned with small, so-called dwarf galaxies. They often contain only a few thousand stars and are 10 to 1000 times smaller than the Milky Way, but they are much more common than large spiral galaxies. The Milky Way is surrounded by at least 60 such galaxies, orbiting their large host as satellites. A similar system is seen around the nearby Andromeda (M31) galaxy, which has at least 27 satellites.

The interesting detail about this host-satellite system is that many of the satellites in each system align in a plane. At fist glance, this might not come as a surprise: The planets in the solar system all orbit in a single plane, and even the Milky Way spiral arms lie within the thin galactic disk. However, these two examples can be explained with our current understanding of physics – the planes of satellites cannot. The standard model of cosmology does not explicitly predict such planes to form, and simulations that were developed to recreate similar systems only rarely produce thin planes.

This tension between theory and observation has created a vivid debate around the topic of planes of satellite galaxies. Some claim that it is a failure of our standard model, suggesting instead theories like "Modified Newtonian Gravity" to replace the assumption of dark matter. Others suggest that the observed systems may have formed this way due to specific factors, like several satellites joining as a group. With limited evidence for any given theory, the question of why planes of satellites form remains unanswered.

This project works with two different sets of simulations to explore the discrepancy between our theory's predictions and the observed reality. One pair of simulations provides a general impression of the results from cosmological simulations. The other set of three simulations is modified to include specific formation events in which the host galaxy merges with another galaxy. This allows us to explore large mergers as a possible explanation for the formation of planes.

Contents

1 Introduction **2**

2 Method **6**
2.1 Simulations 6
2.2 Plane metrics 9
2.3 Satellite selection 10
2.4 Comparison to isotropic distributions 13

3 Results **15**
3.1 Plane height 15
3.1.1 Variable subsets 15
3.1.2 Fixed subsets 17
3.2 Orbital alignment 22
3.2.1 Variable subsets 22
3.2.2 Fixed subsets 22
3.3 Time-variance of planes 23

4 Conclusion **26**
4.1 Variety and rareness of planes 26
4.2 Lifetime of planes 27
4.3 Major mergers as an origin of planes 28
4.4 Summary and outlook 29

A Random subset sampling **35**

Chapter 1

Introduction

The Λ Cold Dark Matter (ΛCDM) model of cosmology has been widely accepted as the standard model thanks to its successes in predicting large-scale structures in the Universe. On a scale much smaller than it was designed for, however, several challenges have been discussed in the study of galactic formation. Specifically, these challenges focus on the dwarf galaxies that are satellites of larger galaxies like the Milky Way or Andromeda. Dwarf galaxies generally have stellar masses in the range of $10^{3-7} M_{\odot}$ and extend across tens of parsecs to a few thousand parsecs (McConnachie, 2012). For comparison, the Milky Way contains roughly 10^{11} stars and has a radius of about 15 kpc (Sparke and Gallagher, 2010).

Some challenges to the ΛCDM model are concerned with the mass and number of dwarf galaxies around larger host galaxies. For example, the "missing satellite problem" relates to the discrepancies between the large number of satellite galaxies predicted by ΛCDM simulations and the relatively small number observed. Somewhat related, the "too big to fail" problem concerns the large number of satellites in dark matter simulations which have such high (dark matter) masses that they would be expected to form stars, with only comparatively few luminous satellites being observed. There is also the "core-cusp problem" in which many simulations predict a steeper increase in dark matter density at the center of galaxies compared to observations (Bullock and Boylan-Kolchin, 2017). These issues have been largely alleviated in recent years by moving from dark-matter-only (DM only) simulations to simulations that also consider baryonic feedback (Garrison-Kimmel et al., 2019). Baryonic feedback refers to processes through which regular, baryonic matter influences galaxy formation. An important example is explosions of massive stars, so-called supernovae. Supernovae drastically change the density and temperature of matter in the surrounding regions and as a result they can lower the efficiency of galactic formation as well as influencing the gravitational potential in dwarf galaxies (Hopkins et al., 2014). When accounting for these feedback effects, simulations more commonly reproduce both the number and mass-density-distribution of the observed satellite galaxies (Garrison-Kimmel et al., 2019).

A more persistent challenge to ΛCDM, however, is the Planes of Satellite Galaxies problem. Our Galaxy, the Milky Way, is surrounded by many small galaxies that are

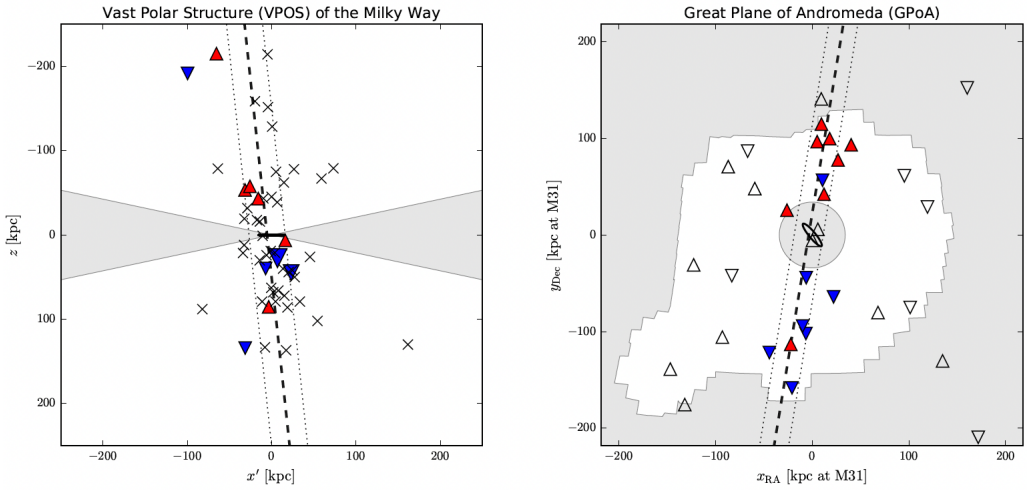

Figure 1.1: The Milky Way and M31 planes of satellites, taken from figure 1 in Pawlowski (2018). The MW system is shown edge-on, M31 as seen from the sun. Red color indicates receding velocities while blue indicates approaching velocities; crosses mark satellites without well-known motion. Non-colored triangles show satellites that are not considered part of the respective plane of satellites. The grey area in the Milky Way image marks the region that is difficult to observe due to being obscured by the galactic disk. In the image for M31, the grey region is the region outside the PAndS survey which provided much of the data.

considered our satellite galaxies, as they are gravitationally bound to the Milky Way. By the 1990's, only 11 such satellites had been discovered – these are now called the "classical satellites". With better observational technology, that number has risen in the past two decades and is currently at around 60 dwarf galaxies (Simon, 2019). When accounting for observational incompleteness, the estimate rises to a total of up to 100-150 satellites (Newton et al., 2018). The most luminous of these seem to align in a planar structure with a root mean square (rms) thickness of 20-30 kpc (Pawlowski, 2018). This is very thin considering that the distances from the center of the Milky Way reach out to around 300 kpc (Metz et al., 2006). The plane is visualized edge-on in the left part of figure 1.1. Furthermore, there appears to be some degree of orbital alignment in the motions of the satellites (Pawlowski, 2018): On average, the angular momentum vectors of the satellites fall within $\sim 60°$ of the mean angular momentum vector.

Andromeda (M31), too, is surrounded by small satellite galaxies. A subset of 15 out of the observed 27 dwarf galaxies forms a thin plane with rms thickness of 12.6 kpc, extending outwards over 400 kpc. This subset and the plane formed by it is shown in the right part of figure 1.1. The subset of 15 satellites was chosen after observing that smaller subsets have a similar plane height but larger subsets appear much less planar (Cautun et al., 2015) – specifically, defining the plane to have 16 members results in a much larger plane height of 50 kpc (Samuel et al., 2021). Thus, this subset was intentionally chosen for forming a thin plane and no other characteristics (such as luminosity or mass) differentiate plane members from non-plane members. Still, the alignment of 15 satellites in such a

thin plane is striking. Furthermore, the alignment of the orbital motions is even more noticeable around M31 than in the set of Milky Way Satellites: 13 out of the 15 considered satellites around Andromeda share the same sense of rotation (that is, counter clockwise or clockwise) (Pawlowski, 2018). An isotropic system would have roughly half of the satellites moving one way or the other. The sense of rotation is visible in the right part of figure 1.1, where most of the satellites above M31 appear to recede, and most below it to approach us.

Many studies have used simulations to test the likelihood of such planes forming. Pawlowski et al. (2014) found that only around 0.2% of dark-matter-only simulations reproduce constellations with similar spatial thinness or orbital coherence as the observed Milky Way. These numbers become even smaller when requiring both aspects simultaneously. Another study, by Samuel et al. (2021), used hydrodynamical simulations (including baryonic feedback) and found comparably thin or orbitally-aligned planes with a noticeably higher frequency of $1 - 5\%$ of simulation snapshots. Still, it seems that ΛCDM simulations, with or without baryonic effects considered, predict a much more isotropic distribution of nearby dwarf galaxies than the one we observe. This discrepancy between a typical simulation result and the observed planes around the Milky Way or Andromeda is what constitutes the "Planes of Satellite Galaxies Problem".

Interpretations of the mentioned simulation results differ. Pawlowski (2018) sees it as a critical flaw in ΛCDM theory that it neither explicitly explains why planes would form, nor typically reproduces observed metrics in simulations. They propose instead a "tidal dwarf theory". In this scenario, the satellites would have been created from tidal interactions of two large galaxies. In a fly-by or collision of two galaxies, the tidal forces can expel some material into a "tidal tail" structure. The displaced gas might then cool and collapse into dwarf galaxies, arranged like "beads on a string" along a tidal tail (Bournaud, 2010). If, for example, the Milky Way collided with another galaxy oriented at a nearly 90° angle to the Milky Way disk, models predict that the tidal tails might form a ring-like structure around the Milky Way (Pawlowski et al., 2012). If regions of the tidal tails collapse into tidal dwarf galaxies, those would then also be located along narrow bands in space. The tidal dwarf theory can thus explain the formation of a highly anisotropic distribution well. However, tidal dwarf galaxies are devoid of dark matter, while the observed satellite galaxies are considered to contain dark matter (Pawlowski, 2018). This, of course, cannot be resolved under the ΛCDM model. Other cosmological models without dark matter have been proposed and support the tidal dwarf theory, such as Modified Newtonian Dynamics (MOND) (Pawlowski et al., 2012).

Other approaches consider special factors that can increase the likelihood of plane formation within ΛCDM cosmology. One explanation, called the group-infall theory, suggests that if several dwarf galaxies were accreted together, it would be expected that they share similar locations and orbital motion (Pawlowski, 2018). Specifically, Samuel et al. (2021) have found that the presence of one particularly heavy satellite, which is often accompanied by more smaller satellites, can increase the likelihood of planes forming. In their study, they found that generally only $\sim 0.3\%$ of their simulations were simultaneously as thin and orbitally coherent as the Milky Way, while $\sim 5\%$ of simulations that include a

satellite comparable to the Large Magellanic Cloud (LMC) fulfill both criteria. Still, in these scenarios the typical number of satellites accreted as a group was between 2 and 4. This small-group-accretion does not fully explain why 14 or more of the Milky Way's satellite galaxies all align in the same plane (Pawlowski, 2018; Samuel et al., 2021). Instead of simply accreting a small group of dwarf galaxies, group-infall theory could also be extended to major mergers in which the merging hosts each bring a number of satellites to the combined system. Indeed, Smith et al. (2016) show that a merger with mass ratio 1:2 can lead to very thin (10-40 kpc) and very stable (over up to 6 Gyr) planes of satellites, if the merger happens under the right conditions. For example, one of the conditions relates to the position of satellites during the merger, as satellites far outside of the plane of the merging event will not form a plane.

Yet another possibility is that the observed plane is merely a temporary alignment, not a meaningful, orbitally stable constellation (Lipnicky and Chakrabarti, 2017). In this interpretation, the rarity of planes in simulations simply means that they are a statistical fluctuation from the more isotropic norm. Alternatively, it can be argued that the small probability of finding Milky Way-like planes in simulations is due to the large variety of planes: The number of satellites considered part of the plane, their orbital motion, and their radial positions are all parameters that influence the plane metrics, thus potentially making a simulated plane with the same height as the Milky Way plane of satellites appear very different (Cautun et al., 2015). Considering this variety could redefine the notion of "rarity" of a plane, as it might be quite common in simulations to find a plane that is highly unlikely to be obtained from an isotropic distribution. By this line of reasoning, many simulated systems are comparable to the observed planar systems of satellites.

All theories for the origins of planes, as well as the varying interpretations of statistics, require further studies to be considered definitive. This project aims to provide additional samples regarding the characteristics of satellite planes found in simulations. We also investigate the influence that the last major merger of the host galaxy may have on the system of satellites. To study the presence or lack of satellite planes, the entire galaxy formation process must be taken into account. Therefore, we use data from five cosmological simulations based on hydrodynamic modelling and considering detailed physics of galaxy formation, including baryonic feedback.

Chapter 2

Method

In this chapter we introduce the five simulations we worked with. We then outline how planes of satellites are quantified by a spatial and a kinematic metric, and how we chose which satellites to consider from each simulation. Lastly, we explain the isotropic systems that we used for comparison with found planar metrics.

2.1 Simulations

Cosmological simulations[1] always start with some initial conditions for the density distribution of matter (sometimes only considering dark matter, sometimes both dark and baryonic matter). Then, the physics defined in the code integrates the system forward in time: All mass particles will exert a gravitational pull on each other and so change the mass distribution, which in some regions leads to collapse of matter into bound structures like galaxies. If baryonic physics is considered then parameters like density thresholds and local temperature are defined to determine when, where, and how star formation and stellar feedback happen. Typically, the initial conditions correspond to the universe at very high redshift (with a near-homogeneous initial mass distribution) and run until around $z \sim 0$ which would correspond to the present time.

Specifically, this work uses a new suite of cosmological simulations, to be presented in Agertz et al. (in prep). To find suitable initial conditions for each halo of interest, a dark matter only simulation was run from $z = 99$ until $z = 0$. This DM only simulation considers a box of size $\sim$ 73 Mpc. It assumes a flat ΛCDM cosmological model and parameters compatible with Planck Collaboration et al. (2016): $\Omega_{\rm m} = 0.3139$, $H_0 = 67.27$, $\sigma_8 = 0.8440$, and $n_s = 0.9645$.

The initial volume for this simulation was created using the GENETIC software (Stopyra et al., 2021). The time evolution was run using the adaptive mesh refinement (AMR) code RAMSES (Teyssier, 2002). Details on this DM simulation can be found in Rey and Starkenburg (2021).

[1] See for example Hopkins et al. (2014) for details on the simulations used in Samuel et al. (2021).

From the results of the DM only simulations, the galactic halos of interest were selected according to the following criteria:

- Milky Way-mass: The virial mass M_{200} contained within r_{200} is $M_{200} \approx 10^{12}$ $M_\odot$ (e.g. Cautun et al. 2020; Deason et al. 2021; see Wang et al. 2020 for a review). Here, r_{200} is the virial radius defined by the enclosed matter having density $\rho = 200\rho_{crit}$, with ρ_{crit} being the critical density of the universe.
- Isolated: There are no other dark matter halos of comparable mass within $5\,r_{200}$.
- Last major merger (LMM): The last major merger happens between 8-10 Gyr before $z = 0$, corresponding to estimates for the Milky Way (Borre et al., 2021).

For each selected halo, a spherical region of radius $3\,r_{200}$ at $z = 0$ was tracked back to the simulation's beginning at $z = 99$. Again using the GENETIC software (Stopyra et al., 2021), the corresponding initial conditions were found with an increased mass resolution[2]. From these zoomed-in initial conditions, the halos of interest could then be resimulated in more detail. This was done using hydrodynamic and N-body code RAMSES. Details on the galaxy formation physics used can be found in Agertz et al. (2021).

The selected halos are named 599, 685, and 715 in the corresponding halo catalogue, and these names will be used throughout this thesis. The snapshots near $z = 0$ that were used from each simulation are shown in figure 2.1. 715 is an elliptical galaxy, 599 a late-type galaxy with an extended disk, and 685 has a smaller and younger disk. They all have stellar masses in the range $2 - 4 \times 10^{10}$ $M_\odot$, similar to the Milky Way (Licquia and Newman, 2015).

Two "genetically modified" versions of halo 685 were also used: 685x09 and 685x12. These differ from 685 in the mass of the last major merger (at $z \sim 2$, or ~ 10 Gyr ago), which was modified to have mass ratio of 1:1, 1:3, and 1:8 for 685x12, 685, and 685x09 respectively. The progenitor to the main halo at the time of the merger has a dark matter halo of mass 2×10^{11} $M_\odot$, and the modified merging galaxies have masses in the range $\sim 5 \times 10^8 - 5 \times 10^9$ $M_\odot$. This agrees with estimates for the galaxy which merged with the Milky Way to form the "Gaia-Enceladus-Sausage" structure (Feuillet et al., 2020).

From the simulations, a halo-finder extracted the positional and velocity data near $z = 0$, which is what we used for our analysis. Usually, only a single snapshot's data was used, but in the case of simulation 715, the analysis was compiled from 11 different snapshots ($\Delta t \approx 341$ Gyr) near $z = 0$.

[2]to particle masses $= 2.3 \cdot 10^5\ M_\odot$

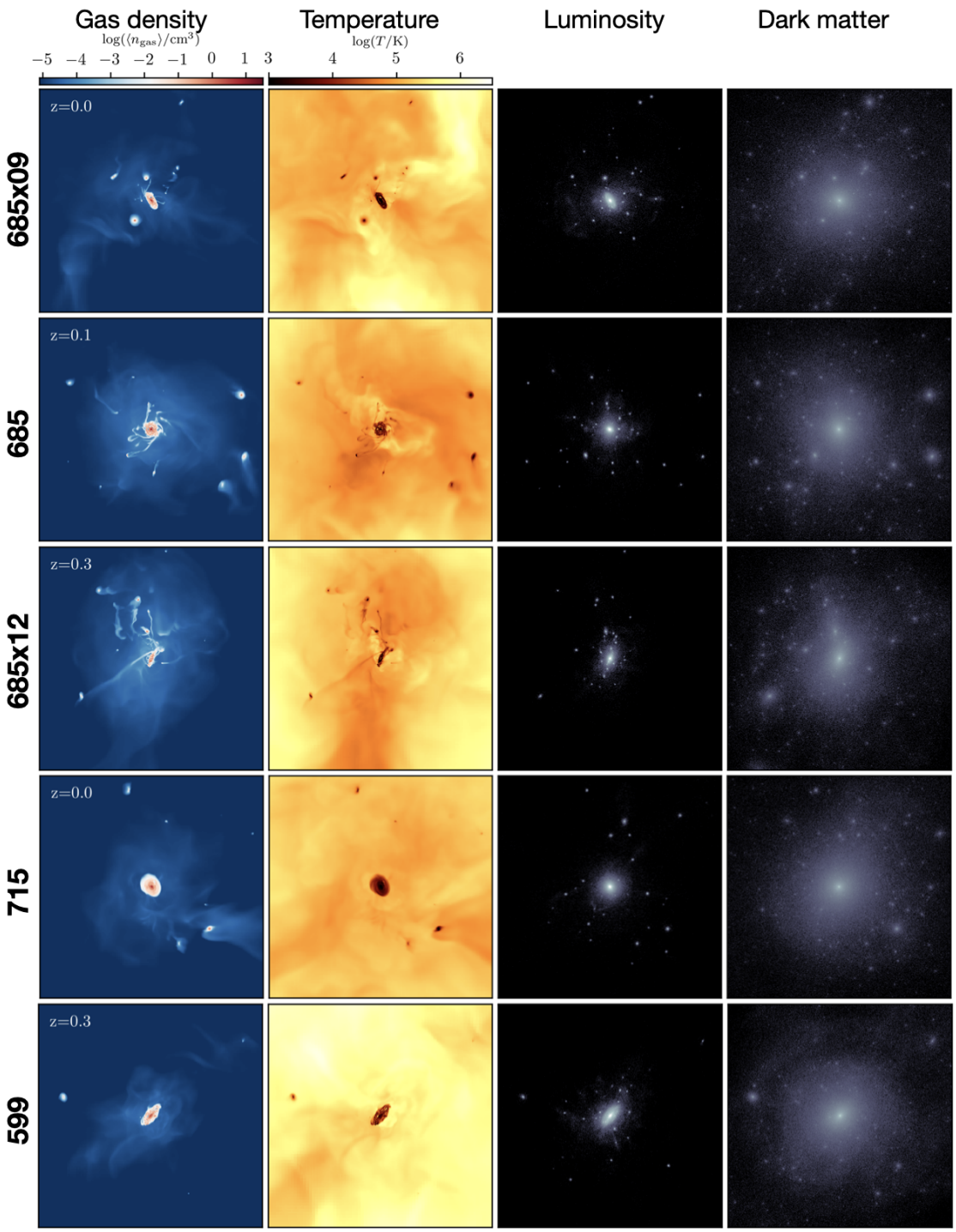

Figure 2.1: Simulation snapshots. The scale of the images is 500 kpc. The luminosity and dark matter density are drawn with arbitrary units. The redshift for each snapshot is noted in the leftmost image.

2.2 Plane metrics

To quantify the planarity of a system with N_{sat} satellites, we use one spatial and one kinematic metric, as is common in the literature. The spatial planarity is characterized by the root mean square (rms) height:

$$\Delta_h = \sqrt{\frac{\sum_{i=1}^{N_{sat}} (d_\perp^2)}{N_{sat}}} \tag{2.1}$$

This is the same formula as equation (1) in Samuel et al. (2021), with $d_\perp$ giving the orthogonal distance from satellite i to the plane. Δ_h is calculated for $2 \cdot 10^3$ different planes[3] with normal vectors evenly sampling the unit sphere. The plane with the smallest rms-height is then considered the plane of best fit to the position sample, and this minimum of Δ_h is cited as the system's rms height. The reason for sampling a large number of planes rather than taking a least-mean-square approach to plane-fitting is that the presented method forces all planes to go through the origin, that is, through the center of the host galaxy. The set of planes is created by choosing x, y, and z values (independently of each other) from a normal distribution and then normalizing them to a unit normal vector[4]:

$$\hat{n} = \frac{1}{\sqrt{x^2 + y^2 + z^2}} \begin{pmatrix} x \\ y \\ z \end{pmatrix} \tag{2.2}$$

Using a finite number of randomly generated plane normal vectors like this introduces an uncertainty, since there is a slight fluctuation in the number of normal vectors per solid angle. Thus, when calculating Δ_h for one system using two different sets of 2000 planes, the result will be slightly different. The variation in measurements for 2000 planes is of the order of 10^{-1} kpc.

To measure how well the motions of satellites align with each other, rms orbital dispersion (Δ_{orb}) is often used. On average, the angular momentum vectors of all plane members will fall within an angle Δ_{orb} of the mean angular momentum vector. This quantity only considers the direction rather than the magnitude of the angular momentum vector. Thus, the vectors considered are the unit vectors for the position, $\hat{n}_{pos} = \vec{r}/|\vec{r}|$, and for the velocity, $\hat{n}_{vel} = \vec{v}/|\vec{v}|$. For each satellite i, the unit angular momentum vector is then calculated as the cross product of position and velocity:

$$\hat{n}_{orb,i} = \hat{n}_{pos,i} \times \hat{n}_{vel,i} \tag{2.3}$$

[3]The choice of using 2000 planes comes from balancing the increased computational time of using a large number of planes with the increased uncertainty of using fewer planes. Samuel et al. (2021) used 10^4 planes to calculate Δ_h, while Cautun et al. (2015) state 10^3 planes in the appendix. Since Δ_{rms} is typically rounded to the nearest integer value in literature, we allowed for the uncertainty of < 0.5 kpc that comes with our choice of 2000 planes.

[4]The code to do this was written with help of Eric Andersson.

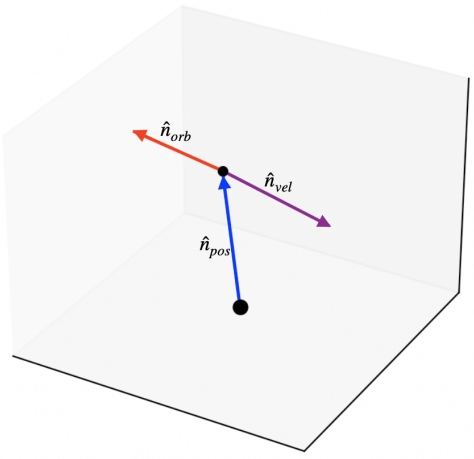

(a) The unit vectors for position and velocity, as well as the angular momentum unit vector $\hat{n}_{orb}$.

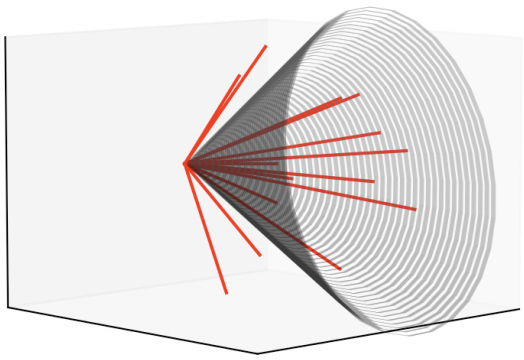

(b) The $\hat{n}_{orb}$ vectors of 14 satellites, as well as a cone with half angle $\Delta_{orb} \approx 52°$ centered around the mean orbital vector. This example is slightly more aligned than the Milky Way system and as such this system would be considered highly orbitally aligned.

Figure 2.2: Illustration of the orbital dispersion

This is illustrated for a sample satellite in figure 2.2a. $\hat{n}_{orb}$ can be seen as the normal vector of the plane in which the satellite orbits the host.

From this set of vectors, the mean orbital vector $\hat{n}_{orb,avg}$ is found by averaging component-wise over all i satellites. The typical angle between the average and an individual vector is calculated as follows:

$$\Delta_{orb} = \sqrt{\frac{\sum_{i=1}^{N_{sat}} (\arccos \hat{n}_{orb,avg} \cdot \hat{n}_{orb,i})^2}{N_{sat}}} \tag{2.4}$$

This is analogous to equation (3) in Samuel et al. (2021). A dispersion of $\Delta_{orb} = 0°$ would mean that all orbital vectors perfectly align and all orbits lie in the same plane. Figure 2.2b pictures Δ_{orb} for an example with 14 satellites.

2.3 Satellite selection

For each host galaxy, we consider only the satellites in a certain range of distances from the host. To exclude any star cluster that lies within the host galaxy (which might be misidentified by the halo finder), all objects within 25 kpc are discarded. This is comparable to the distance from the Milky Way to its nearest satellite galaxy (Kroupa et al., 2005). Any galaxies further than 300 kpc from their host are also discarded, following the parameters used by Samuel et al. (2021). This selection function is similar to the selection of Milky Way satellites (Garrison-Kimmel et al., 2019).

The number of satellites within this region differs between simulations, just as the number of satellites around the Milky Way and around Andromeda are different. Figure

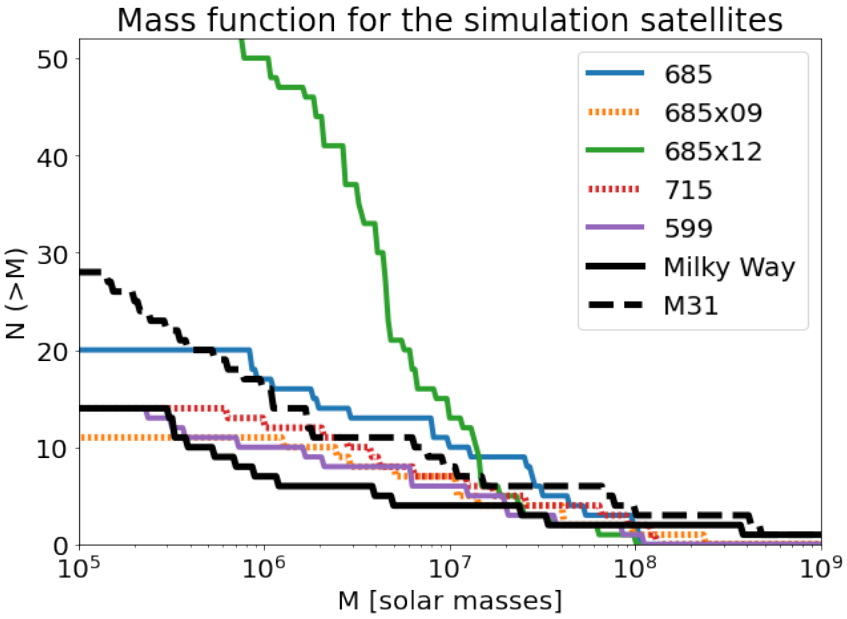

Figure 2.3: Cumulative mass function of the satellites within 25 kpc $<$ d $<$ 300 kpc of the host

2.3 shows the abundance of satellites of different masses in the simulations as well as the two observed systems. The Milky Way and M31 data was adopted from Garrison-Kimmel et al. (2019) and Torrealba et al. (2019).

All simulations have mass functions comparable to both observed systems, falling for the most part in between the Milky Way and Andromeda mass functions. Our simulations are thus realistic representations of a host-satellite system and provide a useful tool for better understanding the systems in the local Universe. 685x12 is the biggest outlier in terms of the mass function: It has a larger number of heavy satellites, meaning that its heaviest 27 satellites are all heavier than $4.5 \cdot 10^6 M_\odot$. Still, the number of very heavy satellites ($\geq 10^7 M_\odot$) in 685x12 is similar to the other simulations and the observed systems. The total number of satellites in the given region ranges from 11 (685x09) to 58 (685x12). The Milky Way plane is generally considered to have 14 satellites in this thesis, while the Andromeda system has 27 satellites.

Our analysis considers two ways to treat these different numbers of N_{sat}: In the first part, N_{sat} is kept variable, testing many different subsets of satellites, while the second part keeps N_{sat} fixed for a more detailed comparison of selected subsets.

The approach of keeping N_{sat} variable is informed by the fact that both the Milky Way and M31 planes include only a subset of the total satellite population. Cautun et al. (2015) raised the criticism that the Great Plane of Andromeda includes only 15 of 27 satellites, and this subset of 15 is not characterized by mass or a similarly clear parameter. Therefore, it is appropriate to consider all possible subsets within a satellite system when searching for planes. This will elucidate the variety of planes that can be defined in any host-satellite system, depending on which dwarf galaxies are considered part of the plane.

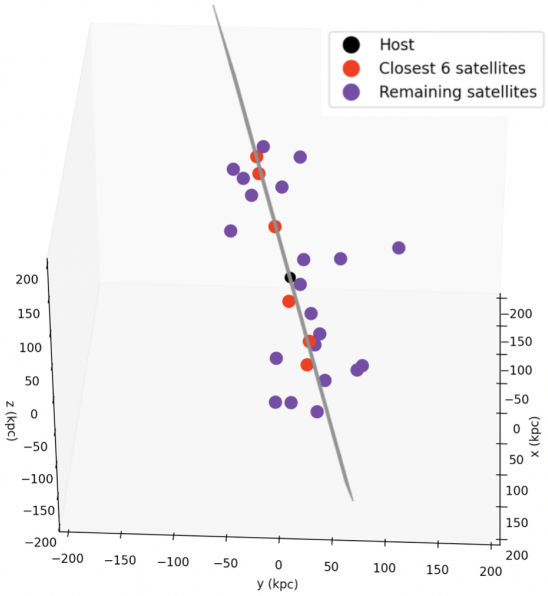

(a) The 6 satellites nearest to a random sample plane (seen edge-on) are marked.

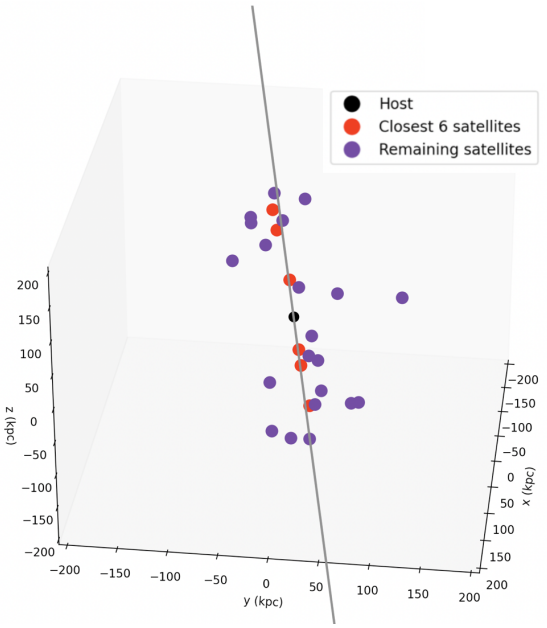

(b) The plane of best fit to this set is calculated, shifting the plane slightly from the one that was used for subset-selection. This example had $\Delta_h = 3$ kpc.

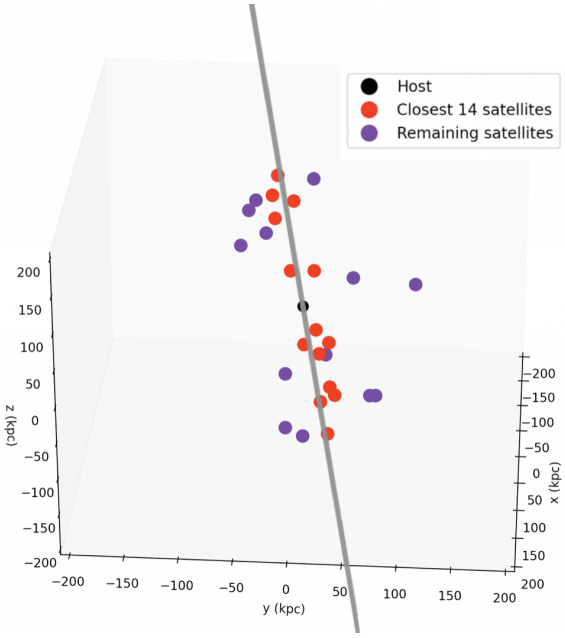

(c) Using the same sample plane as before for subset selection, N_{sat} is increased. Marked here are the 14 satellites closest to the sample plane. This set has $\Delta_h = 7$ kpc.

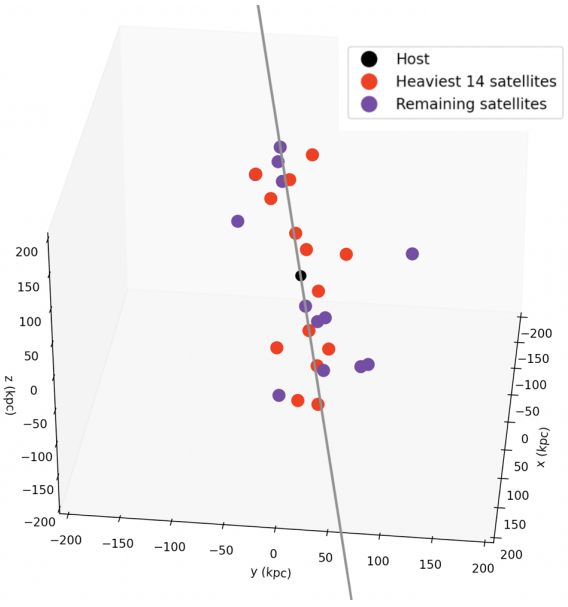

(d) For comparison, this figure shows an alternative method of selecting a subset. The marked satellites are those with the largest mass. This subset has $\Delta_h = 21$ kpc.

Figure 2.4: Subset selection illustration

Similarly to the M31 system, we chose subsets from the list of the 27 heaviest satellites in each system. If the total number of satellite galaxies within the given distance to the host was smaller than 27, all possible satellites were considered.

The number of possible subsets with N_{sat} satellites is immense, especially when $N_{sat} << 27$. To reduce the computational time, Cautun et al. (2015) suggest a method for selecting subsets of satellite galaxies:

- Create a random plane and calculate the distance of each satellite to the plane.
- Order the satellites by distance and choose the $N_{sat} = 6$ satellites[5] that lie closest to the plane as the first subset. See figure 2.4a.
- Calculate the rms height Δ_h and orbital dispersion Δ_{orb} for this subset as described above. See figure 2.4b.
- Increase N_{sat} to include more and more satellites in the subset, and calculate metrics for each set. See figure 2.4c.
- Once $N_{sat} = 27$ is reached (including all considered satellites), create a new random plane. Again, order the satellites by distance and choose subsets for each value of N_{sat}. Repeat the whole process for 1000 random planes. [6]

This method drastically reduces the number of subsets to test while still covering many possibilities that result in thin planes. This bias towards searching for thin planes is justified in the context of the Planes of Satellite Galaxies problem: For each system, only statistically significant or "thin" planes are discussed. After all, it is possible to find less statistically significant planes among subsets of the Milky Way or Andromeda satellites than those that are considered "the" plane of satellite galaxies in each case. Still, while the discussion will focus on the thin planes found, the results from an unbiased, random selection of subsets is provided in the appendix for completeness (figures A.1 and A.2).

The number of satellites included in a plane will of course affect its thickness. In a first step, we merely visualize the range of values obtained from the above method, plotting the plane metrics calculated for each subset. For a more analytical comparison across different values of N_{sat}, one can consider the likelihood to obtain a constellation of satellites with a given Δ_h or Δ_{orb} from isotropic systems.

2.4 Comparison to isotropic distributions

When interpreting planar metrics found for different subsets and varying N_{sat}, it is useful to have an isotropic baseline to compare to. For each subset size N_{sat}, isotropic systems

[5]Cautun et al. (2015) vary N_{sat} starting at 3, but to decrease computational cost, I started subset sampling at $N_{sat} = 6$ instead.

[6]Cautun et al. (2015) stated that using 10^3 planes results in finding a large fraction (70%) of the subsets that were found when using 10^4 planes for subset selection, but using 10^4 planes drastically increased computational time.

with the same number of members were created[7]. The isotropic realizations were generated by randomizing the radial and angular coordinates separately from each other. The radial value r was chosen from a linearly spaced list between 25 and 300 kpc (see the parameters laid out for satellite selection). The direction was randomized by choosing the values for x, y, and z from a normal distribution, then converting them to a unit vector $\hat{n}$ according to equation (2.2), similarly to how the random plane normal vectors were created. The resulting position vector is then simply $\vec{r} = r \cdot \hat{n}$. Thus, both the angular and radial components are fully randomized, but decoupled from each other. The fully randomized comparison is helpful as we understand such statistical distributions better than distributions that depend on simulated parameters.

The radial distribution of a fully randomized scenario will likely be different from the radial values in a simulated or observed system. The radial distribution, of course, has an effect on the planarity of a distribution: A more radially concentrated group of points is more likely to have a small rms height compared to a group at larger radial distances (Cautun et al., 2015). To account for the varying radial distributions, several authors compare to what we will refer to as "semi-randomized distributions" of satellite halos (Samuel et al., 2021). They are still isotropic, since the direction ($\hat{n}$) in which any satellite is found is determined randomly. However, the radial distances (r) are kept the same as in the simulation, making these systems not fully random. Since this method uses the system's radial values, the semi-randomized distribution would have to be calculated for each individual subset of satellites. This is computationally expensive. Therefore, we mainly use this method when analyzing select subsets from each simulation. The probability relative to a semi-randomized distribution is used by Cautun et al. (2015), who define the "prominence" of a plane as the inverse of said probability. We will consider probabilities of $< 5\%$ (or, equivalently, any prominence of > 20) to be statistically significant, in line with the criteria set in Samuel et al. (2021).

The kinetic isotropic analysis randomizes both the position and velocity as described above. Since Δ_{orb} uses only unit vectors, the radial values are irrelevant and there is no distinction between semi and fully randomized systems.

[7]When selecting subsets in simulations, we chose N_{sat} plane members from a total of up to 27 satellites. For time reasons, this was not done in the isotropic scenarios. Instead, these directly consider N_{sat} satellites with randomized positions.

Chapter 3

Results

This chapter presents the findings regarding both the spatial thickness and the orbital dispersion of planes in the simulations. For both metrics, I first explore planes formed from all subsets of satellites chosen via Cautun et al. (2015)'s method (selecting the N_{sat} satellites closest to a test plane) and then the planes of a few specifically selected subsets. The former method is useful both for direct comparison with the Andromeda system and for the discussion of variety and rarity of planes. The more specific plane selection is mostly used for direct comparison with the Milky Way and to examine a few interesting values more closely. Lastly, I show how an example plane of 8 satellites behaves across a time span of 341 Myr to study the longevity of planes.

3.1 Plane height

3.1.1 Variable subsets

We begin by studying the plane heights from all tested subsets in the different simulations. As mentioned before, the Great Plane of Andromeda is often defined with a subset of 15 out of the total 27 satellites – a subset chosen to minimize the plane height (Cautun et al., 2015). Figure 3.1 shows plane heights obtained from a large sample of subsets within our simulations, with the minimal plane height for any given sample size N_{sat} marked by the dotted line. The histograms are column-normalized, so that yellow corresponds to the most common Δ_h-value for each N_{sat}. This was done because the number of possible subsets changes with the size of the subsets, giving each column a different total number of entries. Note that the data for simulation 715 is compiled from 10 different snapshots with a maximum of 14 satellites spanning 341 Myr in simulated time.

For comparison, each plot contains a white dashed line marking the mean value for fully randomized distributions with each value of N_{sat}. While the actual statistical significance was not computed for each subset, intuitively, any histogram entries far away from the isotropic mean can be considered statistically unlikely.

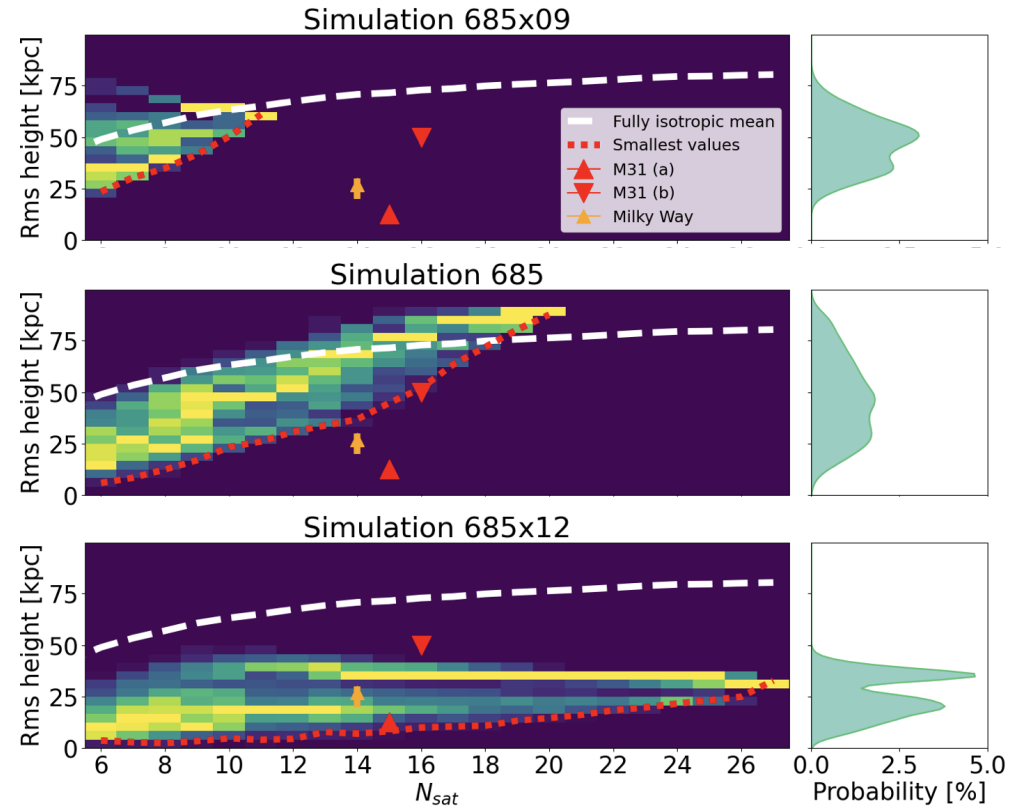

(a) 685-simulations

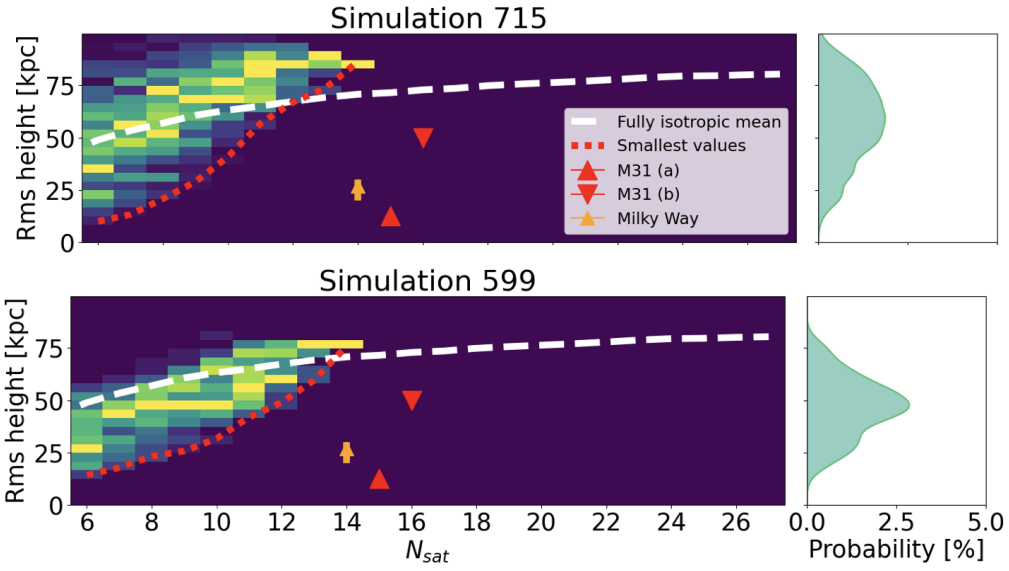

(b) Independent Simulations

Figure 3.1: Heights of the tested subsets in each simulation

Also marked is a range of values for the Milky Way at $N_{sat} = 14$ with $\Delta_{h,MW} = 20 - 30$ kpc (Samuel et al., 2021). For the plane of satellites around the Andromeda galaxy, two values are marked: $\Delta_{h,M31}(a) = 12.5$ kpc (Cautun et al., 2015) and $\Delta_{h,M31}(b) = 50$ kpc (Samuel et al., 2021) from considering $N_{sat} = 15$ and 16 respectively. Each histogram is further accompanied by a projection showing the probability of each rms height value among the samples. This visualizes the range of plane heights when N_{sat} is kept variable.

Generally, all simulations contain a number of planes thinner than the isotropic mean values. Simulation 685 and 685x12 contain planes comparable to the Milky Way and Andromeda, with some subsets in the latter forming planes even thinner than $\Delta_{h,M31}(a)$. The other simulations contain notably fewer satellites in total. This decreases the spread in possible rms heights and makes it less likely to find extremely thin subsets unless the complete set is planar. The full sets from 685x09, 715, and 599 appear more comparable to an isotropic system than to the Milky Way or Andromeda values. Still, it is possible to select a subset with $N_{sat} < N_{total}$ in each simulation that forms a thin plane (see the dotted red lines reaching well below the isotropic mean). The existence of a single such subset is enough to define "the" plane of the system, just as the Great Plane of Andromeda is taken to be the thinnest subset with 15 members (Cautun et al., 2015).

As mentioned earlier, simulations 685x09, 685, and 685x12 form a progression from a fairly small last merger to a heavy last merger. In this progression, is it apparent that the systems become more and more anisotropic. The range of plane heights in system 685 for example extends well below the isotropic mean until higher values of N_{sat} than is the case for 685x09. In 685x12, all planes found are thinner than expected from isotropic distributions. The data levels out towards high values of N_{sat}, showing that the full set of its 27 satellites lie in a single, thin plane. 685x12 is more planar than the Milky Way or the Andromeda system when considering the thinnest subsets.

3.1.2 Fixed subsets

In the case of the Milky Way satellite system, the typically cited plane consists of the $N_{sat} = 14$ heaviest satellites. For a more direct comparison with this scenario, this section will focus on the fixed set of the heaviest 14 satellites in each simulation. To provide further examples, we also discuss the sets with 14 and with 10 members that minimize plane height (that is, the subsets corresponding to the lowest data entries in columns $N_{sat} = 14$ or 10 in figure 3.1).

Figure 3.2 shows the rms height as well as the fully and semi randomized distributions created for each system of the 14 heaviest satellites. The vertical lines in the distributions mark the mean values. 685x09 poses an exception in that it had a maximum of 11 satellites and is compared to a fully randomized distribution with that number of galaxies instead. The Milky Way range of values is again marked in all plots for comparison. We further created a semi-randomized distribution for the Milky Way satellites, which is shown in figure 3.2f. The radial distance data for this was taken from Garrison-Kimmel et al. (2019) and Torrealba et al. (2019), similarly to Samuel et al. (2021).

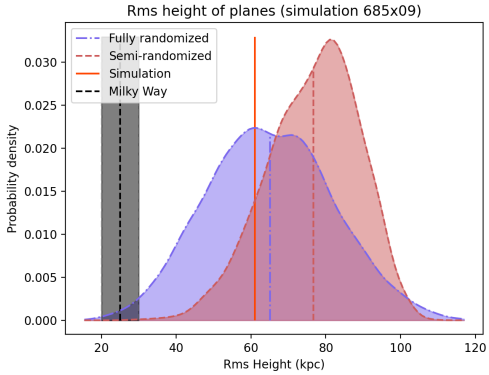

(a) Simulation 685x09 (with $N_{sat} = 11$)

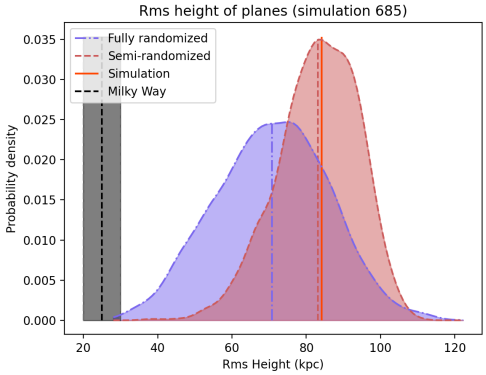

(b) Simulation 685

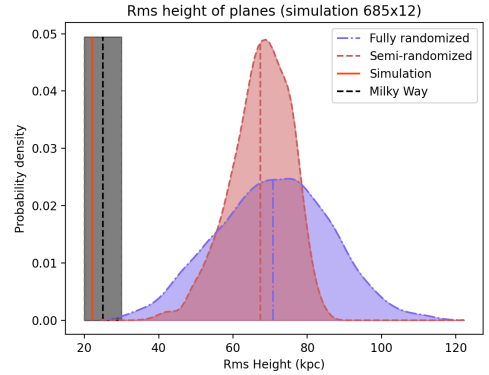

(c) Simulation 685x12

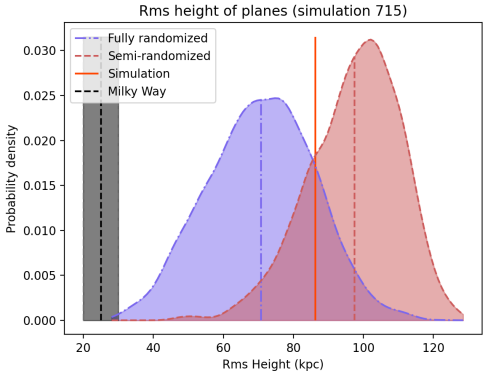

(d) Simulation 715

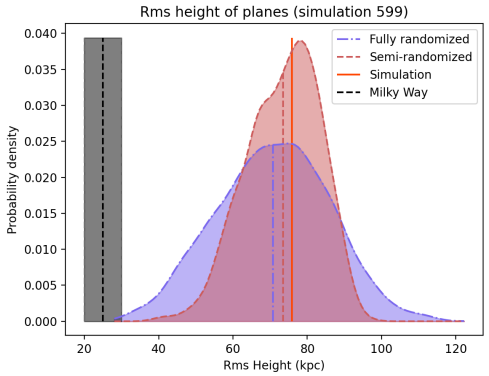

(e) Simulation 599

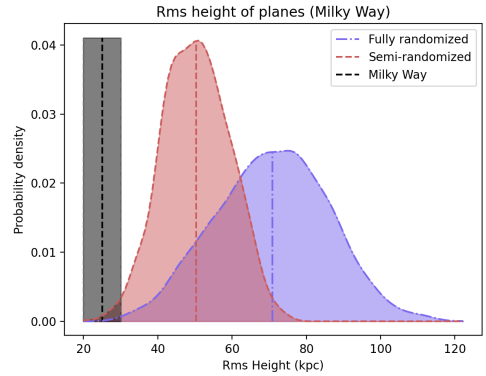

(f) Milky Way

Figure 3.2: The rms height determined for each simulation, shown with the semi-randomized distribution created for that simulation as well as the isotropic distribution for the same parameters.

	Heaviest $N_{sat} = 14$			Thinnest $N_{sat} = 14$			Thinnest $N_{sat} = 10$		
Simulation	Δ_h	Semi	Fully	Δ_h	Semi	Fully	Δ_h	Semi	Fully
685x09[1]	61 kpc	11%	42%	-	-	-	50 kpc	3.9%	24%
685	84 kpc	51%	80%	37 kpc	0.07%	1.3%	24 kpc	0.05%	0.7%
685x12	22 kpc	0%	0.001%	7 kpc	0%	0%	5 kpc	0%	0%
715	86 kpc	20%	84%	-	-	-	47 kpc	0.74%	19%
599	76 kpc	55%	62%	-	-	-	32 kpc	0.3%	3.4%
Milky Way	25 kpc	0.2%	0.01%	-	-	-	-	-	-

Table 3.1: Percentage of semi-randomized or fully randomized isotropic realizations with thinner or equally thin planes as each simulation. The first set of columns corresponds to the set of the 14 heaviest satellites in each simulation (or 11 in the case of 685x09). The second is the thinnest plane with 14 satellites, if it is different from the first set. Lastly, the thinnest plane with 10 satellites. Subsets were chosen from up to 27 satellites, as in the previous section. Entries of "0%" were approximated from results of $< 10^{-4}$%.

Table 3.1 lists the percentage of planes in each random distribution that had an rms height of less or equal to that found for the simulation. This computation was done for all three mentioned sets (where applicable): The 14 (or 11, for 685x09) heaviest satellites, the 14 satellites minimizing plane height, and the 10 satellites minimizing plane height. Here, a percentage of $< 50\%$ implies that the simulation is more planar than would be expected from an isotropic distribution. Visually, this simply corresponds to the simulation value lying to the left of the indicated mean values in figure 3.2. Following Samuel et al. (2021), we will consider any plane with a fraction of $< 5\%$ to be significant. These values are marked red in the table.

The only difference between the fully and semi-randomized methods is the radial distribution. To better understand this effect, figure 3.3 shows the cumulative radial distribution of the Milky Way as well as the simulations. The grey background is the spread of 1000 fully randomized realizations, with the black line marking the isotropic mean.

Clearly, the Milky Way satellites are more radially concentrated than most isotropic distributions. Generally, a more radially concentrated group of points will be expected to give a smaller rms height, hence why the semi-randomized distribution in figure 3.2f is centered around a lower mean than the fully randomized distribution. Meanwhile, simulation 715 for example has no satellites at distances below 100 kpc and is thus noticeably less radially concentrated. This explains the shift towards higher rms heights in its semi-randomized distribution.

As a result, while simulation 715 seems not very planar when judging purely by plane height and is well within the expected values for an isotropic distribution, it turns out that it is anisotropic when accounting for the radial distribution. This simply means that a system with all satellites quite far away from the host galaxy is unlikely to be as planar as simulation 715 is. Meanwhile, the fact that the Milky Way satellites are more radially concentrated is not enough to explain the thinness of the observed plane, since the statistical significance persists even when comparing to semi-randomized realizations.

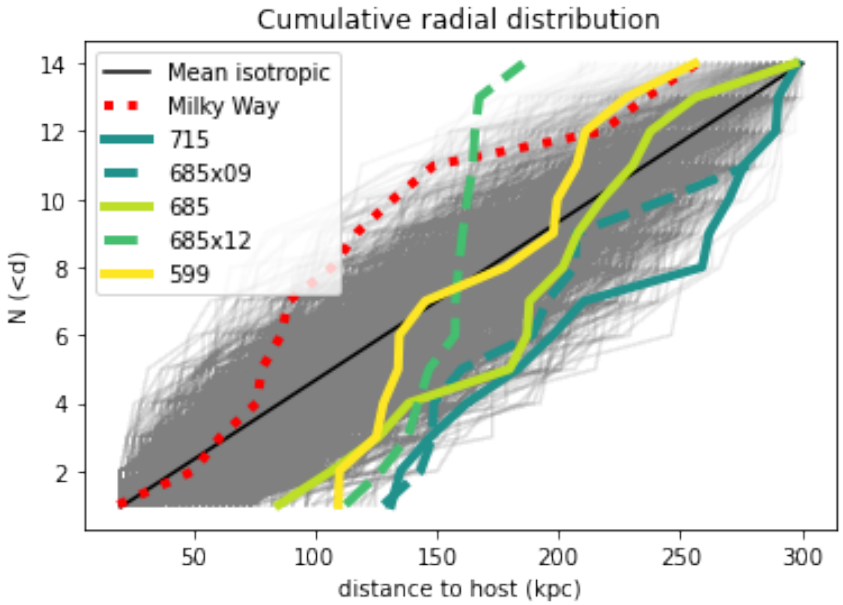

Figure 3.3: Number of satellites (of the 14 heaviest) within distance d of the host. The gray background shows the spread of 1000 random realizations

Out of the sets of the heaviest satellites, only simulation 685x12 has a plane thin enough to be considered statistically significant. It is thinner than the Milky Way plane and even more prominent than the Milky Way plane when considering its radial distribution. Simulations 685 and 599 match closely the expectation values (with probabilities near 50%). Simulations 685x09 and 715 appear insignificant relative to a fully randomized distribution, but due to their radial distribution lying further out than the isotropic mean, they are somewhat rare in semi-randomized scenarios.

When choosing subsets to minimize the plane height, every simulation contains a statistically significant plane. Among the set of 685-simulations, the plane height as well as the isotropic probability decrease from 685x09 to 685x12 when considering 10 satellites. This corresponds to the general trend observed in figure 3.1a.

It is important to keep in mind that detecting a single significant plane in any given simulation is enough to consider that simulation planar, unless specific conditions are imposed on the definition of satellite planes (such as only allowing subsets consisting of the heaviest N_{sat} satellites in a system). Thus, each of our simulations can be seen as planar and planar configurations of satellites appear to be common.

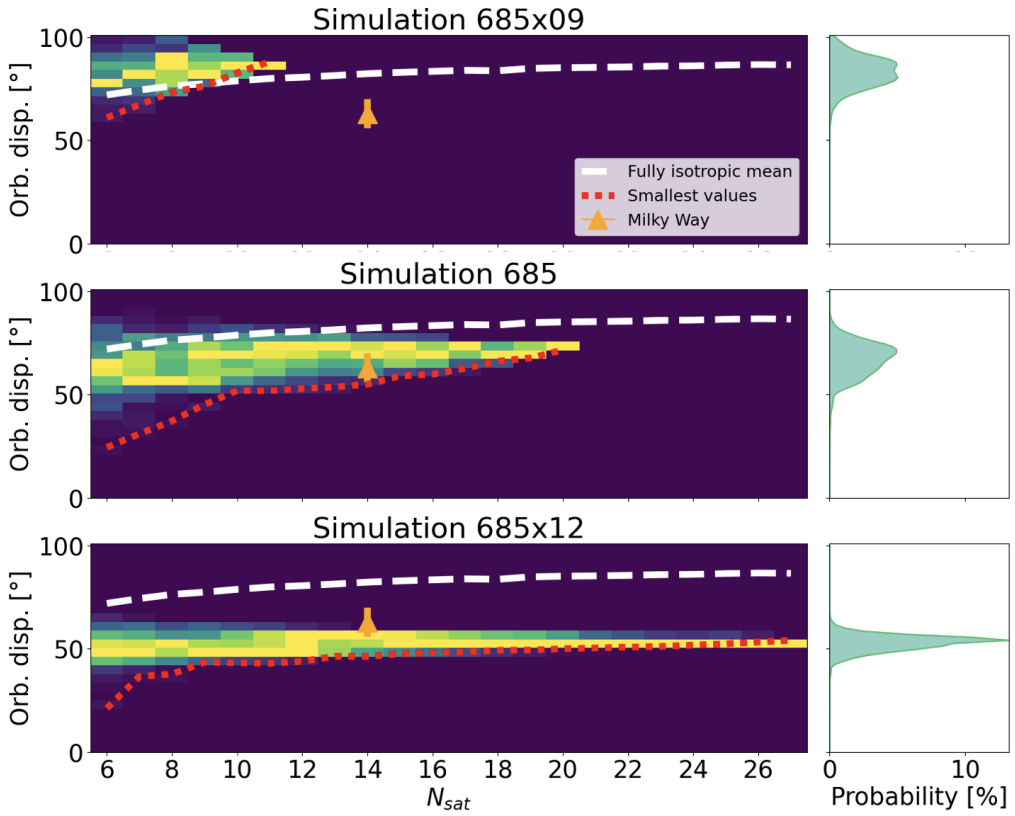

(a) 685-simulations

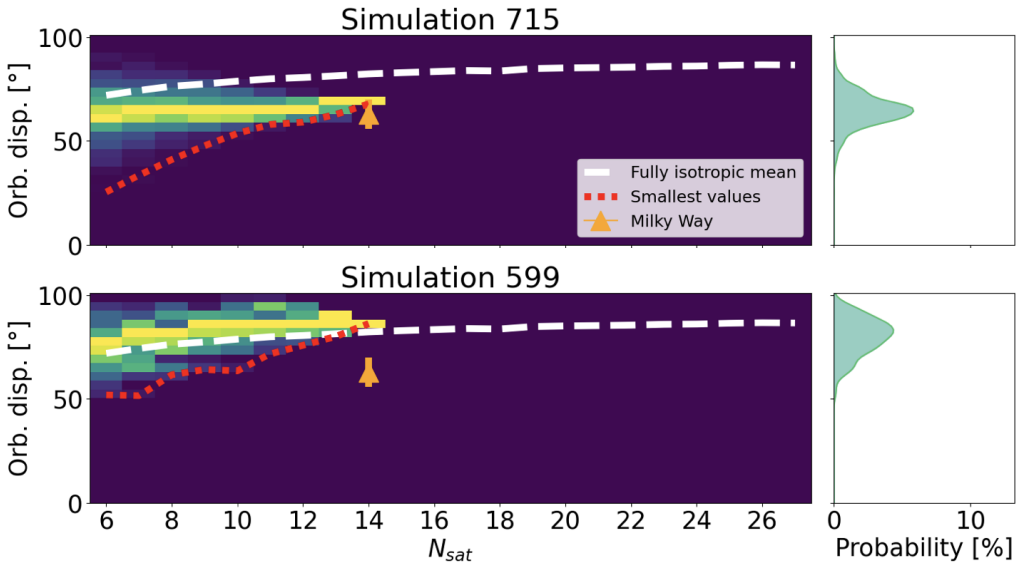

(b) Independent Simulations

Figure 3.4: Orbital dispersion of the tested subsets in each simulation

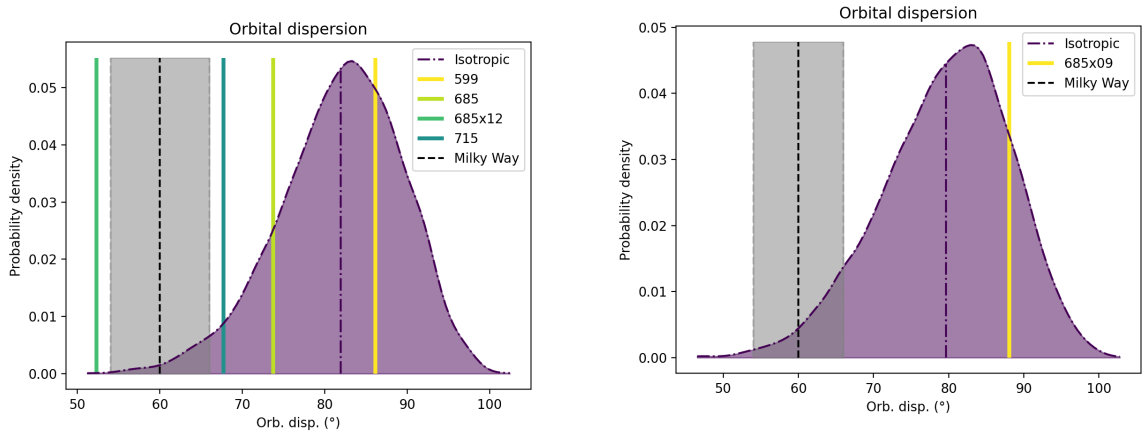

(a) All simulations with $N_{sat} = 14$

(b) Simulation 685x09 compared to isotropic realizations with $N_{sat} = 11$

Figure 3.5: Orbital dispersion of the 14 (or 11) heaviest satellites in each simulation

3.2 Orbital alignment

3.2.1 Variable subsets

Figure 3.4 shows the equivalent to figure 3.1 for orbital dispersion. Again, the dashed line shows the mean value from isotropic distributions, the dotted line the measured minima, and the orange marker shows the orbital dispersion of the Milky Way plane of satellites at about $\Delta_{orb,MW} = 54 - 66°$ (Samuel et al., 2021). Only line-of-sight velocity data is available for the M31 satellites, so orbital dispersion cannot be calculated for that system.

Out of the shown systems, 599 and 685x09 appear the least orbitally aligned – generally even less so than an average isotropic system, with only a few exceptions of more aligned subsets. Simulation 685 and 715 lie below the isotropic mean and show values comparable to the Milky Way system. Simulation 685x12 stands out as the only simulation with values of $\Delta_{orb} < 50°$, and $\Delta_{orb} \approx 50°$ even at large N_{sat}. This is more orbitally coherent than the Milky Way satellites.

3.2.2 Fixed subsets

As before, we will also compare the orbital dispersion of the simulations to the Milky Way under the condition of using the 14 heaviest satellites as a fixed set. Again, simulation 685x09 is compared to an isotropic distribution of 11 satellites instead. The orbital dispersion of each set, as well as that of the Milky Way, are shown in figure 3.5 over a background of an isotropic distribution. Table 3.2 then lists the corresponding orbital dispersions and the probability associated with each value relative to the isotropic distribution.

All simulations except 599 in figure 3.5a lie below the isotropic mean, implying that the systems are somewhat orbitally aligned. However, the isotropic distribution is quite broad

and both simulations 599 and 685 fall relatively close to the isotropic mean. Simulation 685x12, just as in the spatial metrics, lies towards the very tail of the random distribution, even more so than the Milky Way values. Simulation 685x09 is again the least orbitally coherent.

	Heaviest $N_{sat} = 14$		Min. $N_{sat} = 14$		Min. $N_{sat} = 10$	
System	Δ_{orb}	Probability	Δ_{orb}	Probability	Δ_{orb}	Probability
685x09	88°	84%	-	-	83°	62%
685	74°	14%	55°	0.004%	52°	0.9%
685x12	52°	0.0001%	46°	0%	43°	0.1%
715	68°	3.8%	-	-	54°	1.2%
599	86°	70%	-	-	64°	7%
MW	60°	0.3%	-	-	-	-

Table 3.2: Orbital dispersion and the cumulative likelihood of obtaining each value from an isotropic system. The first results describe the subsets of the 14 (or 11, for 685x09) heaviest satellites; then the most orbitally aligned with $N_{sat} = 14$ and 10 respectively.

Table 3.2 further lists the orbital dispersion and associated isotropic probability for the sets minimizing Δ_{orb} in each simulation, given $N_{sat} = 14$ and $N_{sat} = 10$. As expected from the distributions in figure 3.4, all simulations except for 685x09 have subsets that are much more orbitally aligned than expected from an isotropic distribution. Still, only simulations 685 and 685x12 contain subsets that are as statistically significant as the Milky Way plane (for the chosen values of N_{sat}, at least).

3.3 Time-variance of planes

To explore the development of planes over time, we considered 11 different snapshots of simulation 715. This covers a time span of around 341 Myr. The most obvious development across these snapshots is that the number of satellites in the region between 25 and 300 kpc varies. Snapshots 0-3 have between 12 and 14, while snapshots 4-7 only have 9 satellites in total. Later, in snapshots 8-10, the number increases to 11 again. With one exception, this appears to be due to the halo finder not always identifying all of the smaller galaxies. The exception is from snapshots 3 to 4, where one satellite crosses the distance of 300 kpc to the host and is subsequently no longer considered in our analysis. In future work, improved halo finding will be prioritized.

The movement of the satellites is visualized in figure 3.6a. Satellites that disappeared between snapshots are recognizable as pale points without direct trace to a clearly visible point. The velocities of the satellites range from around 55 to 110 km/s. In 340 Myr, this corresponds to a movement of around 20-40 to kpc.

The movement of the satellites will of course affect the planarity of the system. For a direct comparison across snapshots, we selected a subset of 8 satellites that were present in all snapshots, traced through time via position, approximate mass, and a continuous

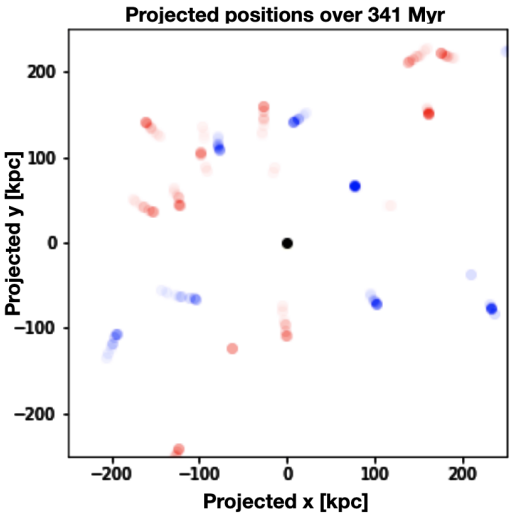

(a) Visualization of the movement of satellites

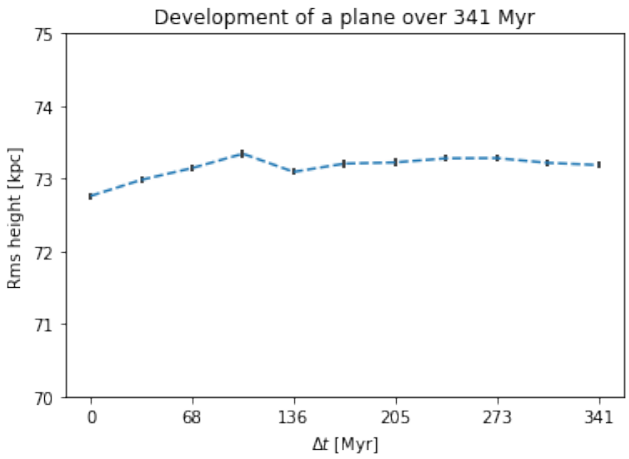

(b) Plane height Δ_h

Figure 3.6: Development of simulation 715 across 11 snapshots spanning 341 Myr: (a) shows the movement across the 11 snapshots. The palest markers are the positions in the earliest snapshot, the clearest markers from the last snapshot. Blue color indicates satellites that are at a radial distance beyond 300 kpc from the host and thus not considered in the analysis. The black dot marks the host galaxy. (b) shows the plane height of a subset that was traced throughout all snapshots.

change in each satellite's speed. The rms height corresponding to this subset is shown in figure 3.6b. Since the variation in Δ_h is of the order of 0.1 kpc, we increased the number of planes used to determine the plane of best fit in order to decrease the uncertainty in our calculated rms height to be of the order of 0.01 kpc. The plotted error bars are a high estimate of the uncertainties. There appears to be no monotonic trend. The maximum variance in the plane height here is around 0.6 kpc.

The isotropic mean height for 8 satellites lies at 57 kpc, the semi-isotropic mean calculated at one of the snapshots is 93 kpc (as simulation 715 generally is less radially concentrated than an average system, see figures 3.3 and 3.2d). The semi-isotropic probability lies around 14 %, making the considered system not statistically significant by our previous definition, but certainly more planar than an isotropic system.

The orbital dispersion across these snapshots is constantly near 61°. This is about as aligned as the Milky Way system, although of course $N_{sat} = 8$ in this case, making a higher alignment more statistically likely than in the case of the Milky Way. Intuitively, the approximate motion of 20-40 kpc over the considered time would be expected to have a stronger impact on the plane height than the measured variance of 0.6 kpc, although a more detailed analysis would be needed to better understand the degree of orbital alignment.

From these results, it can be said that the given plane persists over 341 Myr. This is less time than it would typically take for a satellite to complete an orbit, as orbital periods range from 1 to ∼4 Gyr depending on the radial distance to the host (Samuel et al., 2021).

However, with no clear trend indicating that the plane is beginning to dissolve during the considered time interval, the plane is likely not "transient". Samuel et al. (2021) define constellations lasting less than 500 Myr as transient, and those over 1 Gyr as "long-lived". More snapshots would need to be considered to make a statement about how long-lived the plane in simulation 715 is, which we leave for a future investigation.

Chapter 4

Conclusion

In this chapter, we discuss our results in the context of other studies. We also interpret the trends observed in the set of modified simulations (685x09, 685, and 685x12) with regards to the mergers in the formation history of each system. At this point, we compare to previous findings pertaining to merger processes, the tidal dwarf theory, and group infall.

4.1 Variety and rareness of planes

As shown in figures 3.1 and 3.4, the considered simulations contain a large variety of planes, with each data point representing a different combination of number of satellites, radial distribution, plane height, and orbital alignment. Tables 3.1 and 3.2 show that every simulation contains some plane that is highly statistically unlikely compared to isotropic distributions. This aligns with the findings from Cautun et al. (2015) stating that statistically unlikely planes are not rare in simulations. Some of our simulations even contain planes that are more statistically significant than the Milky Way plane. This is despite the fact that all simulations also contain planes that appear not unlike isotropic systems, supporting the importance of evaluating the prominence (or statistical likelihood) of planes.

When a more rigid method of selecting subsets is applied, our simulation results generally appear less planar than the Milky Way system. Specifically, we selected the heaviest 14 satellites in each simulation to agree with a common definition of plane-members among the Milky Way satellites (Samuel et al., 2021). Out of the five simulations we analyzed, only 685x12 was notably planar when considering this specific selection. This agrees with common findings stating that only around $1-5$ percent simulation snapshots appear very planar (Pawlowski, 2018; Samuel et al., 2021). Similarly, 685x12 is the only system where this fixed subset is more orbitally aligned than the Milky Way satellites. However, the situation is not as extreme in this metric as in the spatial metric: System 715 for example has an orbital dispersion only slightly higher than the maximum value cited for the Milky Way. Again, this is in agreement with previous findings. For example, Samuel et al. (2021) show in figure 2 that, while only around 5% of their simulations were more aligned than the Milky Way system, the number quickly rises at only slightly higher values of Δ_{orb}, with

quite a few simulations having nearly as small values as the Milky Way.

Simulation 685x12 is special in that it contains a number of planes that are both thinner and more statistically significant than the Milky Way plane (see table 3.1). Samuel et al. (2021) noted that some of their simulated systems had plane thicknesses comparable to the Milky Way, but none were as statistically significant. Furthermore, simulation 685x12 simultaneously has $\Delta_h < \Delta_{h,MW}$ and $\Delta_{orb} < \Delta_{orb,MW}$, which other studies have found in only around $0.2\% - 0.3\%$ of their simulations (Pawlowski, 2018; Samuel et al., 2021). It remains to be seen what is the cause for this discrepancy.

4.2 Lifetime of planes

Only one of the simulation was analyzed across several snapshots. This example plane had plane height $\Delta_h \approx 73$ kpc and orbital dispersion of $61°$. Its statistical significance compared to a semi-randomized system lies at $\sim 14\%$, classifying it as somewhat but not extremely planar. Both the spatial and orbital metrics stayed fairly constant across 11 snapshots, spanning a time of approximately 340 Myr, with no clear indicator that the plane height will change drastically just outside of this time span.

Other studies have considered the lifetime of planes over a much longer time span. Bahl and Baumgardt (2014) for example show that the lifetimes of the planes found in their dark matter simulations are short (< 1 Gyr), making thin planes a momentary alignment rather than a stable orbital structure. Two factors make it difficult to compare their results directly with ours: The rms height of their short-lived plane is much smaller than that of simulation 715, and their plot of $\Delta_h(t)$ only plots data points at approximately 0.5 Gyr intervals. The simulations considered by Bahl and Baumgardt (2014) typically had rms heights from 20-100 kpc across ~ 10 Gyr, except for a span of ~ 1 Gyr where the heights drop below 14 kpc. Simulation 715 never reaches such small values of Δ_h in the given snapshots. Here it would be useful to know the statistical significance of the planes in Bahl and Baumgardt (2014) – the radial distribution of 715 specifically makes thin planes less likely than in the other simulations, so the semi-randomized probability would be useful in judging whether system 715 is comparable to those in the study and would be expected to behave similarly over time. In their figure 10 it appears quite obvious that such extremely thin planes are only temporary alignments. Due to the limited number of data points plotted, however, it is unclear how the slope of $\frac{\Delta_h}{t}$ looks in detail, that is, whether their systems show periods of strong alignment that look as constant as figure 3.6b. This makes it difficult to estimate whether the shown state of 715 would be expected to change drastically in a time span beyond the considered snapshots.

Samuel et al. (2021) also considered the lifetime of planes by comparing simulation snapshots across ~ 5 Gyr. Similarly to Bahl and Baumgardt (2014), this study considered the life time of a plane to be the time span for which a system has a height below a certain threshold ($\Delta_h < 28$ kpc for "Milky-Way like" planes and $\Delta_h < 48$ kpc for "generic" planes). By this definition, many of their simulations only show such thin planes in one snapshot (corresponding to a lifetime of < 25 Myr) and only very few have life times longer than

1 Gyr. Among their longest-lived planes are the systems containing an LMC-analogue. Again, the plane considered for simulation 715 does not fall under the given rms height threshold and would not be counted as a relevant plane in this study, despite being more statistically significant than some of the systems considered in Samuel et al. (2021).

All this is to say that several studies show that thin planes only rarely have long lifetimes, but these studies typically only consider planes selected by means of Δ_h. As discussed above, the fact that statistically significant planes come in a wide variety (with different values of N_{sat}, Δ_h, Δ_{orb}, and radial distributions) can be used to argue that even planes with a large absolute plane thickness (a large value of Δ_h) should be considered as relevant examples of planes in simulations, if they are unlikely to be obtained from semi-randomized realizations. Therefore, it would be interesting to consider snapshots of simulation 715, as well as the other simulations, across a longer time window to see if statistically unlikely formations will persist across longer times than those found by the aforementioned studies. From the limited amount of data we analyzed, it seems possible that the relevant plane in simulation 715 might be longer lived than the planes typically found in other studies, but this is purely a guess based off a small number of snapshots.

4.3 Major mergers as an origin of planes

When considering simulations 685x09, 685, and 685x12, there is a clear trend in both spatial and kinematic metrics: System 685x09 is the least planar, 685x12 is significantly planar, and 685 falls between the two. This is clear both from the absolute values of Δ_h and Δ_{orb}, as well as from the statistical significance of selected subsets (see tables 3.1 and 3.2).

The order from least to most planar corresponds to the order of the mass ratio in the last major merger. When creating the simulations, halo 685x09 was modified to have a mass ratio of 1:8 for its last major merger; the ratios were 1:3 for 685 and 1:1 for 685x12. Thus, a larger merger appears to correlate to a thinner plane of satellites.

There is another trend, independently of plane metrics: The total number of satellites in the considered region is smallest in 685x09 and largest in 685x12. Since the satellites were not tracked throughout the formation history of the systems, it is impossible to say how many of the satellites were brought in by the merging galaxy. It is further unknown where the different satellites were located at the time of the merger, which might be an important factor for plane formation according to Smith et al. (2016). As a first guess, Smith et al. (2016)'s findings suggest that the large merger and the additional satellites that come with it are likely to be the main reason for the strong alignment seen in 685x12. It would be interesting to explore the parameters Smith et al. (2016) identified as making systems more planar, such as the positions of satellites relative to the plane of the merger.

By the Tidal Dwarf Theory advocated by Pawlowski et al. (2012) it would also be possible that a larger merger, with stronger tidal forces, could create more tidal dwarfs. However, figure 2.1 seems to show that the considered satellites in our simulations also contain dark matter and can therefore not be tidal dwarfs. A more detailed analysis of the

dark-matter content as well as the formation history of the satellites would be needed to make a definitive statement on this.

Furthermore, simulation 685x12 also contains more heavy satellites than the other simulations, as seen in figure 2.3. This might relate to Samuel et al. (2021)'s findings that the presence of a very heavy satellite (an LMC-analogue) makes thin planes much more likely than they are in systems without such a satellite. No direct comparison between our systems and their findings is possible: They only considered galaxies with $M_\star > 10^9 M_\odot$ to be LMC-analogues, which none of our simulations' satellites fulfills. Interestingly, the most massive satellite in simulation 685x09 is heavier ($2.4 \cdot 10^8 M_\odot$) than the heaviest satellite in simulations 685 or 685x12 ($\sim 1 \cdot 10^8 M_\odot$). Still, the presence of a larger number of heavy satellites in 685x12 might have a similar gravitational effect to the single extremely heavy LMC-analogue in Samuel et al. (2021)'s study. The stronger gravitational pull could possibly have a stabilizing effect on the plane. Again, due to the limited data used in our analysis, this is merely a guess.

With regards to group infall, a detailed analysis of the number of dwarfs accreted in groups is given in Shao et al. (2018). They find from hydrodynamical simulations that massive satellites are singly accreted in $\sim 75\%$ of cases, and about 14% in pairs. Samuel et al. (2021) generally agree with these findings but point out LMC-analogues as special cases: They state that the main reason why systems including an LMC are more planar than others is because the LMC-analogue is typically accompanied by several other dwarfs. Based on these studies, with 685x12 having no LMC-analogue but many heavy satellites, plane members would be expected to be individually or pair-accreted, with larger groups being highly unlikely. Additionally, even systems with LMC-group accretion typically only bring 2-4 additional dwarfs to the system, which can only account for a part of the final set of plane members (Samuel et al., 2021). Therefore, group accretion outside of the major merger probably cannot fully explain the extreme planarity of 685x12, although further investigation is needed.

4.4 Summary and outlook

This project worked with five MW-mass systems from cosmological simulations, which were run considering detailed galaxy-formation physics. Three of the simulations were modified to include mergers of set mass ratios at look-back time ~ 10 Gyr, comparable to estimates for the Milky Way formation history. The findings regarding planarity of the satellite systems can be summarized as follows:

- Planar structures show a large diversity regarding the number of plane members N_{sat}, their radial distribution, plane height, and orbital dispersion. The statistical likelihood of obtaining a given plane from a semi-randomized distribution is a highly relevant metric when interpreting simulation results, as it makes different systems more comparable.

- All simulations contain statistically significant planes (compared to semi-randomized

systems), showing that statistically unlikely planes are not uncommon in simulations. Some of the considered planes are more statistically significant than the Milky Way system. While only a fraction of all the planes we identified fall into this category, it is sufficient to find a single such plane in any system to consider it "the" plane of the system.

- Simulation 685 contains planes comparable in N_{sat} and Δ_h to the thicker of the values used for the Andromeda system (with $\Delta_h \approx 50$ kpc at $N_{sat} = 16$). Simulation 685x12 contained planes that were thinner than the Milky Way or Andromeda planes of satellites at the same value of N_{sat}. Essentially all planes in 685x12 are more orbitally aligned than the Milky Way system.

- An exemplary plane was found to have a near-static plane height and orbital dispersion across 341 Myr. While this could possibly point towards a longer lifetime of the plane, it is difficult to compare to findings in other studies due to the different selection criteria used for planes.

- Among the suite of modified simulations, a heavier last major merger corresponded to a more planar system. Furthermore, the system with the heaviest merger had more and more heavy satellites than the other systems.

The findings regarding the last major merger need to be backed up by a larger sample size, but point towards a possible causation. The details of the processes causing thinner planes can only be speculated about at this point. More work needs to be done to pinpoint the origins of the planes, including studying the dynamics of the merger, large-scale accretion, and whether the plane members differ from any off-plane satellites.

Our method has limitations and can not be seen as a perfect representation of the Universe. The simulations have limited resolutions and work with simplified physics (such as ignoring black hole feedback). The halo finder is also not entirely reliable in identifying satellite galaxies, as became clear when comparing different snapshots of the same simulation. Moreover, our methods for selecting subsets of satellites as well as plane-fitting should be run with more repetitions to increase the accuracy. Most importantly, the analysis should be performed on a much larger sample of simulations and more snapshots from each simulation. This would both make the results more reliable, as outliers due to halo-finding issues would have a smaller effect, and make our results statistically representative. From the small number of simulations considered, we can not estimate how common such planes are in simulations in general, merely that they exist in a few cases.

Based purely on my samples, we do not find a strong tension between the observed MW and M31 systems and ΛCDM simulations. However, we do identify many possibilities for future work, including analyzing more simulations and tracking them over a longer time span, as well as investigating the details of how the last major merger influences plane formation.

Bibliography

Agertz, O., Renaud, F., Feltzing, S., Read, J. I., Ryde, N., Andersson, E. P., Rey, M. P., Bensby, T., and Feuillet, D. K. (2021). VINTERGATAN - I. The origins of chemically, kinematically, and structurally distinct discs in a simulated Milky Way-mass galaxy. *MNRAS*, 503(4):5826–5845.

Bahl, H. and Baumgardt, H. (2014). A comparison of the distribution of satellite galaxies around Andromeda and the results of ΛCDM simulations. *MNRAS*, 438(4):2916–2923.

Borre, C. C., Aguirre Børsen-Koch, V., Helmi, A., Koppelman, H. H., Nielsen, M. B., Rørsted, J. L., Stello, D., Stokholm, A., Winther, M. L., Davies, G. R., Hon, M., Kruijssen, J. M. D., Laporte, C., Reyes, C., and Yu, J. (2021). Age Determination of Galaxy Merger Remnant Stars using Asteroseismology. *arXiv e-prints*, page arXiv:2111.01669.

Bournaud, F. (2010). Tidal dwarf galaxies and missing baryons. *Advances in Astronomy*, 2010:1–7.

Bullock, J. S. and Boylan-Kolchin, M. (2017). Small-Scale Challenges to the ΛCDM Paradigm. *ARA&A*, 55(1):343–387.

Cautun, M., Benítez-Llambay, A., Deason, A. J., Frenk, C. S., Fattahi, A., Gómez, F. A., Grand, R. J. J., Oman, K. A., Navarro, J. F., and Simpson, C. M. (2020). The milky way total mass profile as inferred from Gaia DR2. *MNRAS*, 494:4291–4313.

Cautun, M., Bose, S., Frenk, C. S., Guo, Q., Han, J., Hellwing, W. A., Sawala, T., and Wang, W. (2015). Planes of satellite galaxies: when exceptions are the rule. *MNRAS*, 452(4):3838–3852.

Deason, A. J., Erkal, D., Belokurov, V., Fattahi, A., Gómez, F. A., Grand, R. J. J., Pakmor, R., Xue, X.-X., Liu, C., Yang, C., Zhang, L., and Zhao, G. (2021). The mass of the Milky Way out to 100 kpc using halo stars. *MNRAS*, 501(4):5964–5972.

Feuillet, D. K., Feltzing, S., Sahlholdt, C. L., and Casagrande, L. (2020). The SkyMapper-Gaia RVS view of the Gaia-Enceladus-Sausage - an investigation of the metallicity and mass of the Milky Way's last major merger. *MNRAS*, 497(1):109–124.

Garrison-Kimmel, S., Hopkins, P. F., Wetzel, A., Bullock, J. S., Boylan-Kolchin, M., Kereš, D., Faucher-Giguère, C.-A., El-Badry, K., Lamberts, A., Quataert, E., and Sanderson, R. (2019). The Local Group on FIRE: dwarf galaxy populations across a suite of hydrodynamic simulations. *MNRAS*, 487(1):1380–1399.

Hopkins, P. F., Kereš, D., Oñorbe, J., Faucher-Giguère, C.-A., Quataert, E., Murray, N., and Bullock, J. S. (2014). Galaxies on FIRE (Feedback In Realistic Environments): stellar feedback explains cosmologically inefficient star formation. *MNRAS*, 445(1):581–603.

Kroupa, P., Theis, C., and Boily, C. M. (2005). The great disk of Milky-Way satellites and cosmological sub-structures. *A&A*, 431:517–521.

Licquia, T. C. and Newman, J. A. (2015). Improved estimates of the milky way's stellar mass and star formation rate from hierarchical bayesian meta-analysis. *The Astrophysical Journal*, 806(1):96.

Lipnicky, A. and Chakrabarti, S. (2017). Is the vast polar structure of dwarf galaxies a serious problem for Λ cold dark matter? *MNRAS*, 468(2):1671–1682.

McConnachie, A. W. (2012). The Observed Properties of Dwarf Galaxies in and around the Local Group. *AJ*, 144(1):4.

Metz, M., Kroupa, P., and Jerjen, H. (2006). The spatial distribution of the Milky Way and Andromeda satellite galaxies. *Monthly Notices of the Royal Astronomical Society*, 374(3):1125–1145.

Newton, O., Cautun, M., Jenkins, A., Frenk, C. S., and Helly, J. C. (2018). The total satellite population of the Milky Way. *MNRAS*, 479(3):2853–2870.

Pawlowski, M. S. (2018). The planes of satellite galaxies problem, suggested solutions, and open questions. *Modern Physics Letters A*, 33(6):1830004.

Pawlowski, M. S., Famaey, B., Jerjen, H., Merritt, D., Kroupa, P., Dabringhausen, J., Lüghausen, F., Forbes, D. A., Hensler, G., Hammer, F., and et al. (2014). Co-orbiting satellite galaxy structures are still in conflict with the distribution of primordial dwarf galaxies. *Monthly Notices of the Royal Astronomical Society*, 442(3):2362–2380.

Pawlowski, M. S., Pflamm-Altenburg, J., and Kroupa, P. (2012). The VPOS: a vast polar structure of satellite galaxies, globular clusters and streams around the Milky Way. *MNRAS*, 423(2):1109–1126.

Planck Collaboration, Ade, P. A. R., Aghanim, N., Arnaud, M., Ashdown, M., Aumont, J., Baccigalupi, C., Banday, A. J., Barreiro, R. B., Bartlett, J. G., Bartolo, N., Battaner, E., Battye, R., Benabed, K., Benoît, A., Benoit-Lévy, A., Bernard, J.-P., Bersanelli, M., Bielewicz, P., Bock, J. J., Bonaldi, A., Bonavera, L., Bond, J. R., Borrill, J., Bouchet,

F. R., Boulanger, F., Bucher, M., Burigana, C., Butler, R. C., Calabrese, E., Cardoso, J.-F., Catalano, A., Challinor, A., Chamballu, A., Chary, R.-R., Chiang, H. C., Chluba, J., Christensen, P. R., Church, S., Clements, D. L., Colombi, S., Colombo, L. P. L., Combet, C., Coulais, A., Crill, B. P., Curto, A., Cuttaia, F., Danese, L., Davies, R. D., Davis, R. J., de Bernardis, P., de Rosa, A., de Zotti, G., Delabrouille, J., Désert, F.-X., Di Valentino, E., Dickinson, C., Diego, J. M., Dolag, K., Dole, H., Donzelli, S., Doré, O., Douspis, M., Ducout, A., Dunkley, J., Dupac, X., Efstathiou, G., Elsner, F., Enßlin, T. A., Eriksen, H. K., Farhang, M., Fergusson, J., Finelli, F., Forni, O., Frailis, M., Fraisse, A. A., Franceschi, E., Frejsel, A., Galeotta, S., Galli, S., Ganga, K., Gauthier, C., Gerbino, M., Ghosh, T., Giard, M., Giraud-Héraud, Y., Giusarma, E., Gjerløw, E., González-Nuevo, J., Górski, K. M., Gratton, S., Gregorio, A., Gruppuso, A., Gudmundsson, J. E., Hamann, J., Hansen, F. K., Hanson, D., Harrison, D. L., Helou, G., Henrot-Versillé, S., Hernández-Monteagudo, C., Herranz, D., Hildebrandt, S. R., Hivon, E., Hobson, M., Holmes, W. A., Hornstrup, A., Hovest, W., Huang, Z., Huffenberger, K. M., Hurier, G., Jaffe, A. H., Jaffe, T. R., Jones, W. C., Juvela, M., Keihänen, E., Keskitalo, R., Kisner, T. S., Kneissl, R., Knoche, J., Knox, L., Kunz, M., Kurki-Suonio, H., Lagache, G., Lähteenmäki, A., Lamarre, J.-M., Lasenby, A., Lattanzi, M., Lawrence, C. R., Leahy, J. P., Leonardi, R., Lesgourgues, J., Levrier, F., Lewis, A., Liguori, M., Lilje, P. B., Linden-Vørnle, M., López-Caniego, M., Lubin, P. M., Macías-Pérez, J. F., Maggio, G., Maino, D., Mandolesi, N., Mangilli, A., Marchini, A., Maris, M., Martin, P. G., Martinelli, M., Martínez-González, E., Masi, S., Matarrese, S., McGehee, P., Meinhold, P. R., Melchiorri, A., Melin, J.-B., Mendes, L., Mennella, A., Migliaccio, M., Millea, M., Mitra, S., Miville-Deschênes, M.-A., Moneti, A., Montier, L., Morgante, G., Mortlock, D., Moss, A., Munshi, D., Murphy, J. A., Naselsky, P., Nati, F., Natoli, P., Netterfield, C. B., Nørgaard-Nielsen, H. U., Noviello, F., Novikov, D., Novikov, I., Oxborrow, C. A., Paci, F., Pagano, L., Pajot, F., Paladini, R., Paoletti, D., Partridge, B., Pasian, F., Patanchon, G., Pearson, T. J., Perdereau, O., Perotto, L., Perrotta, F., Pettorino, V., Piacentini, F., Piat, M., Pierpaoli, E., Pietrobon, D., Plaszczynski, S., Pointecouteau, E., Polenta, G., Popa, L., Pratt, G. W., Prézeau, G., Prunet, S., Puget, J.-L., Rachen, J. P., Reach, W. T., Rebolo, R., Reinecke, M., Remazeilles, M., Renault, C., Renzi, A., Ristorcelli, I., Rocha, G., Rosset, C., Rossetti, M., Roudier, G., Rouillé d'Orfeuil, B., Rowan-Robinson, M., Rubiño-Martín, J. A., Rusholme, B., Said, N., Salvatelli, V., Salvati, L., Sandri, M., Santos, D., Savelainen, M., Savini, G., Scott, D., Seiffert, M. D., Serra, P., Shellard, E. P. S., Spencer, L. D., Spinelli, M., Stolyarov, V., Stompor, R., Sudiwala, R., Sunyaev, R., Sutton, D., Suur-Uski, A.-S., Sygnet, J.-F., Tauber, J. A., Terenzi, L., Toffolatti, L., Tomasi, M., Tristram, M., Trombetti, T., Tucci, M., Tuovinen, J., Türler, M., Umana, G., Valenziano, L., Valiviita, J., Van Tent, F., Vielva, P., Villa, F., Wade, L. A., Wandelt, B. D., Wehus, I. K., White, M., White, S. D. M., Wilkinson, A., Yvon, D., Zacchei, A., and Zonca, A. (2016). Planck 2015 results. XIII. Cosmological parameters. *A&A*, 594:A13.

Rey, M. P. and Starkenburg, T. K. (2021). How cosmological merger histories shape the diversity of stellar haloes. *arXiv e-prints*, page arXiv:2106.09729.

Samuel, J., Wetzel, A., Chapman, S., Tollerud, E., Hopkins, P. F., Boylan-Kolchin, M., Bailin, J., and Faucher-Giguère, C.-A. (2021). Planes of satellites around Milky Way/M31-mass galaxies in the FIRE simulations and comparisons with the Local Group. *MNRAS*, 504(1):1379–1397.

Shao, S., Cautun, M., Frenk, C. S., Grand, R. J. J., Gómez, F. A., Marinacci, F., and Simpson, C. M. (2018). The multiplicity and anisotropy of galactic satellite accretion. *MNRAS*, 476(2):1796–1810.

Simon, J. D. (2019). The Faintest Dwarf Galaxies. *ARA&A*, 57:375–415.

Smith, R., Duc, P. A., Bournaud, F., and Yi, S. K. (2016). A Formation Scenario for the Disk of Satellites: Accretion of Satellites during Mergers. *ApJ*, 818(1):11.

Sparke, L. S. and Gallagher, J. S. (2010). *Galaxies in the universe: an introduction*. Cambridge Univ. Press.

Stopyra, S., Pontzen, A., Peiris, H., Roth, N., and Rey, M. P. (2021). GenetIC—A New Initial Conditions Generator to Support Genetically Modified Zoom Simulations. *ApJS*, 252(2):28.

Teyssier, R. (2002). Cosmological hydrodynamics with adaptive mesh refinement. A new high resolution code called RAMSES. *A&A*, 385:337–364.

Torrealba, G., Belokurov, V., Koposov, S. E., Li, T. S., Walker, M. G., Sanders, J. L., Geringer-Sameth, A., Zucker, D. B., Kuehn, K., Evans, N. W., and Dehnen, W. (2019). The hidden giant: discovery of an enormous Galactic dwarf satellite in Gaia DR2. *MNRAS*, 488(2):2743–2766.

Wang, H. F., López-Corredoira, M., Huang, Y., Carlin, J. L., Chen, B. Q., Wang, C., Chang, J., Zhang, H. W., Xiang, M. S., Yuan, H. B., Sun, W. X., Li, X. Y., Yang, Y., and Deng, L. C. (2020). Mapping the Galactic disc with the LAMOST and Gaia red clump sample: II. 3D asymmetrical kinematics of mono-age populations in the disc between 6-14 kpc. *MNRAS*, 491(2):2104–2118.

Appendix A

Random subset sampling

Throughout the thesis, subsets of satellites were selected using the method suggested by Cautun et al. (2015). This introduces a bias towards thinner planes, which is desirable when searching for significant planes. For completeness, the results from random subset sampling are provided on the following pages. Notably, the bias towards thinner planes does not always correspond to more orbitally aligned planes. Thus, the results from random selection include some subsets that are more orbitally aligned than those found with Cautun et al. (2015)'s method. The difference between the two methods is quite small, however, so this was not further discussed in the thesis.

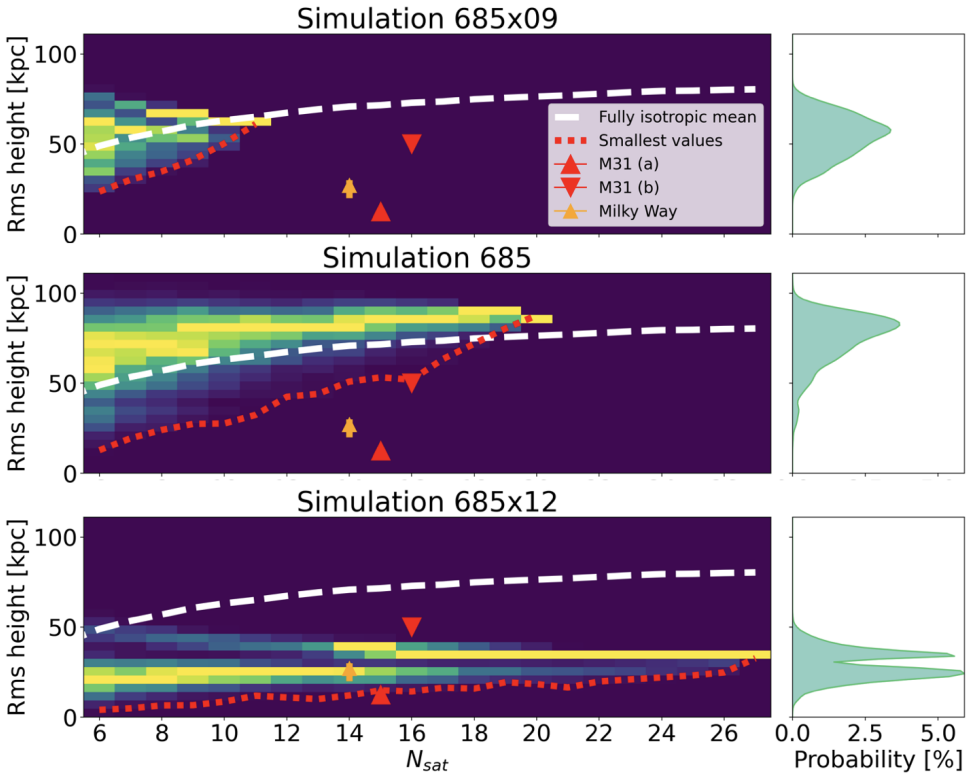

(a) 685-simulations

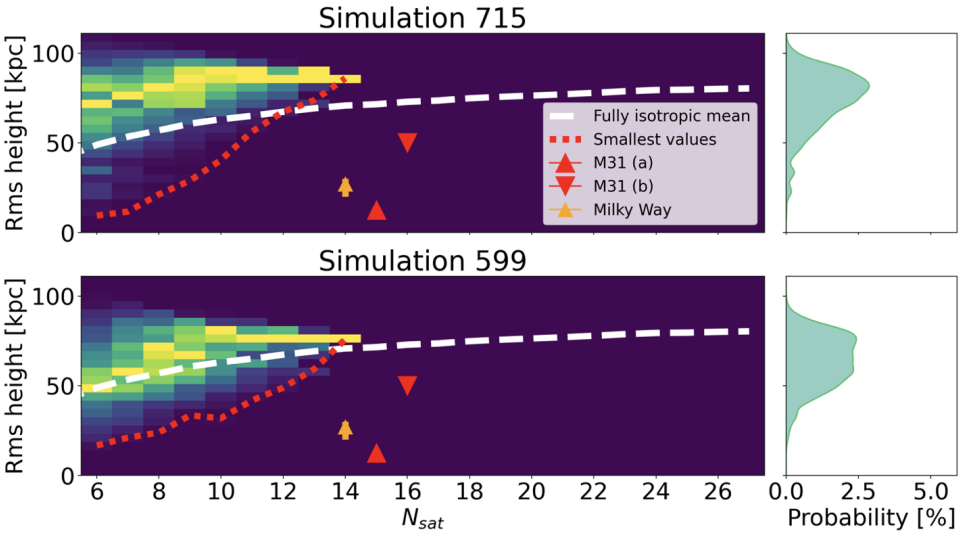

(b) Independent Simulations

Figure A.1: Plane heights of a number of randomly selected subsets

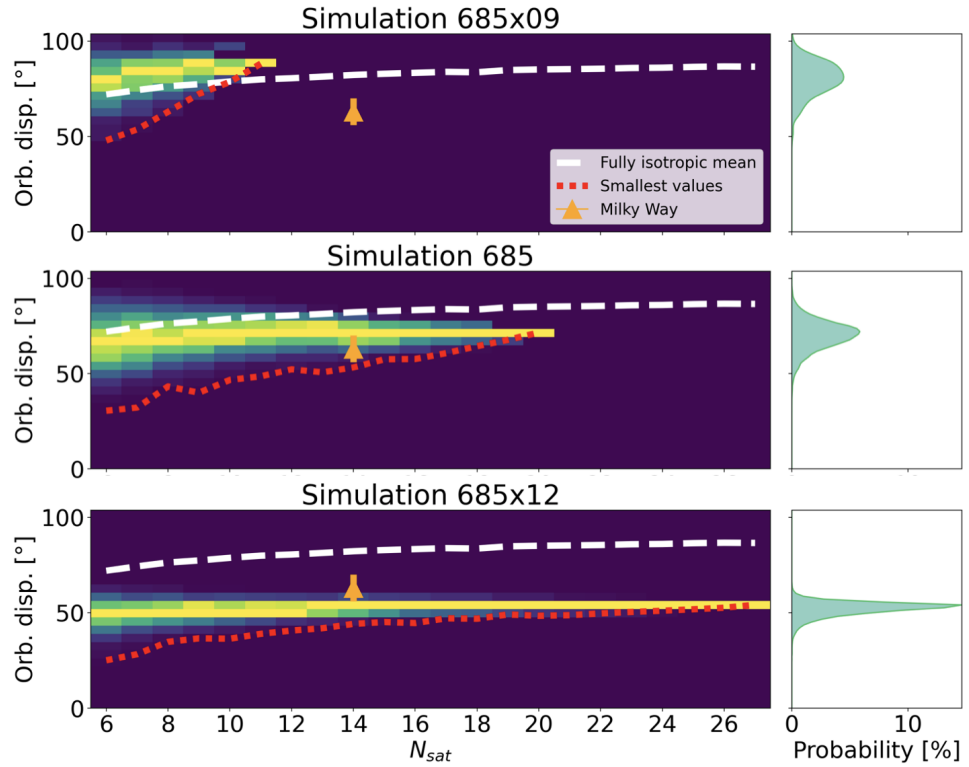

(a) 685-simulations

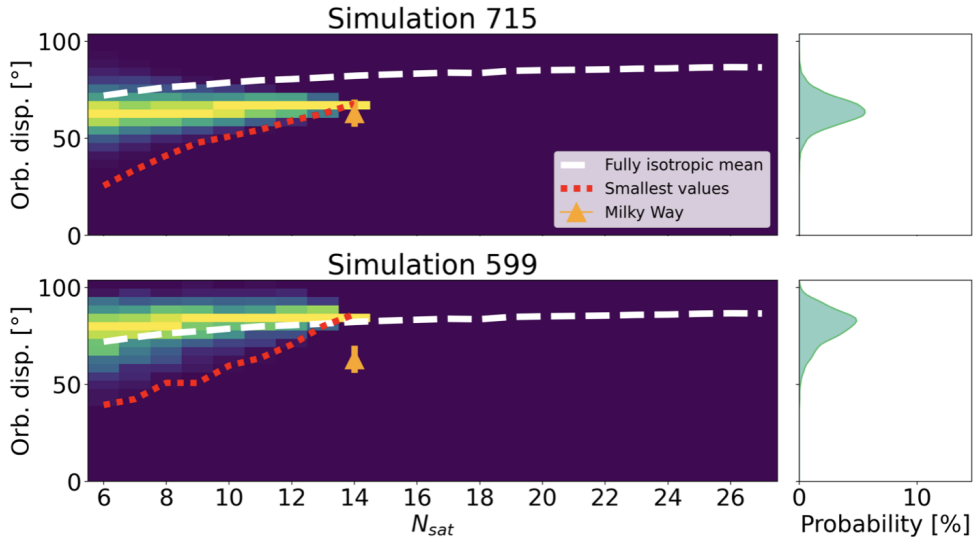

(b) Independent Simulations

Figure A.2: Orbital dispersion of a number of randomly selected subsets